MICROSCOPY

1. Introduction

There are many excellent textbooks available that thoroughly discuss each form of microscopy. The goal of this article is to provide a broad review of the various types of microscopes. Emphasis is placed on basic concepts, applications, the type of information obtained, and the advantages and disadvantages of each type of microscopy. Throughout this article, acronyms will be used to denote both the technique (microscopy) and the instrument (microscope). See Appendix I for a list of all acronyms used.

Microscopy involves the production and study of magnified images of objects too small to resolve with the unaided eye. There is no single type of microscope; rather, there are dozens, having in common only the ability to present an enlarged image. Microscopes may be categorized based on the mechanism by which the enlarged image is formed. For example, light microscopes utilize visible, ultraviolet (uv) or infrared (ir) electromagnetic radiation (ie, light) to illuminate and/or stimulate the sample. Furthermore, the light may be polychromatic "white" or monochromatic (eg, laser). In a light microscope, conventional glass lenses are used to provide magnification and the light is either transmitted through the sample or reflected off its surface. Light microscopes are perhaps the most versatile because they can be used to examine almost any type of sample (eg, living, moving, solid, liquid, or gas) and under almost any conditions of temperature or pressure. This flexibility in the operating environment makes light microscopes ideal for *in situ* observations of living processes and chemical reactions. Microscopes are commonly used to measure properties or observe qualities such as, size, shape, texture, color, absorption wavelengths, reflectance, crystallinity, melting point, refractive index, dispersion, fluorescence, interference phenomena, chemical composition, and many other physical and chemical properties (Table 1).

Other types of microscopes employ electromagnetic lenses or slits to collimate a beam of electrons, ions, or X-rays that are used to illuminate or stimulate the sample. Microscopes of this type are commonly referred to as "electron microscopes", "ion microscopes", and "X-ray microscopes", respectively. As the beam is scanned across the sample, a variety of signals are emitted from the point of beam impact (eg, secondary electrons, backscatter electrons, Auger electrons, sample ions, X-rays). To form an image, the intensity of the signal is plotted as a function of the beam's instantaneous XY position. To increase magnification, it is only necessary to reduce the area of the scan. Light microscopes may also be operated in this fashion, ie, with a scanned beam of light. As with light microscopes, electron microscopes may transmit the electron beam through the sample as in transmission electron microscopy (TEM) or reflect the beam off the sample surface as in scanning electron microscopy (SEM). In electron microscopes, the images obtained may be of extremely high resolution ($<$0.5 nm) and are often extremely realistic owing to their high depth of field. However, electron, ion and X-ray images lack color information and may not be immediately suitable for imaging any type of sample. For example, specimens that are in motion, wet, or electrically insulating may yield unacceptable images or may be damaged by the instruments vacuum environment or intense beam. However, recent

advancements in SEM have produced a "high pressure" SEM (HPSEM), also known as the environmental SEM (ESEM) or variable pressure SEM (VPSEM), that is able to produce high resolution images without a vacuum and on nearly any sample, including wet samples. This advancement has virtually eliminated two of the most significant drawbacks to using SEM.

Another widely used form of microscope is the scanning probe microscope (SPM). This microscope comes in two major varieties, the scanning tunneling microscope (STM) and the atomic force microscope (AFM). Even though the SPM has only been commercially available since ~1986, their use has become widespread. SPMs accomplish microscopic imaging in a manner completely unlike previous microscopes. An image of the sample surface is formed by mapping out the spatial position of an extremely fine probe as it is being rastered just a few nanometers above the sample surface. As the probe is rastered over an area of known lateral dimensions, the electrical current (STM) or atomic forces (AFM) that extend away from the sample cause the probe to be deflected toward or away from the surface. In AFM, these minute vertical deflections of the probe are detected by an optical lever technique and plotted with respect to the probe's instantaneous X,Y position, thus producing a three dimensional (3D) map of a specific sample property. Depending on the type of probe being utilized or the particular "mode" of operation, it is possible to map out a wide variety of sample properties such as surface microtopography, surface magnetic field, surface chemical qualities, hardness, and conductance to name but a few. This wide range of potential characterization data and the ability of the SPM to resolve single atomic sites on almost any material and while operating in almost any environment (eg, air, fluid, vacuum) make the SPM more versatile than most types of microscopes.

Other forms of microscopes may utilize sound waves, radio waves, or phonons to accomplish microscopic imaging. No matter what type of microscope is being considered, it is beneficial for the operator to always keep in mind the nature of both the input signal(s) used to illuminate or stimulate the sample and also the output signal(s) being detected by the eye or other detector. Although a thorough understanding of the theory of a particular form of microscopy is usually not necessary to be a user, this knowledge will greatly reduce the risk of misinterpreting an image and will also add to the quality and efficiency with which images and data are collected.

Since light, electron, and scanning probe microscopes are by far the most commonly used microscopes, they are discussed in greater detail in this article. Table 1 provides a brief summary of some of capabilities, advantages, disadvantages, and cost of these three most common types of microscopes. Note that because microscopes vary drastically in terms of quality and added features, ranges are given for most of the values in Table 1.

Given that each type of microscope will always have certain advantages/disadvantages over other types, it is proper to regard the various microscopes as complimentary rather than competitive. Each microscopical technique was designed with a specific purpose in mind, such as providing improved spatial resolution or more types of characterization data. As the field of microscopy has evolved, it has not been possible to develop a single microscope that simultaneously achieves the best performance in all categories (eg, spatial resolution,

temporal resolution, depth of field, characterization data, detection limit, and flexibility in operating environment). Instead, new microscopes are invented with new or improved capabilities. However, oftentimes new capabilities are achieved only at the expense of other features. For example, electron microscopes and SPMs offer an $\sim 1000\times$ increase in spatial resolution over light microscopes, but both achieve this improved resolution with undesirable tradeoffs. For example, most electron microscopes require at least a low vacuum to support the electron beam and the sample must be conductive enough to dissipate the electrical current the beam delivers. These requirements restrict the application of SEM to nonliving specimens. Because tradeoffs will always exist between different forms of microscopy, the microscopist should be familiar with the strengths and weaknesses of each technique so that he/she can decide which technique(s) will provide the best characterization data for a particular sample. Of course, it should be pointed out that good microscopes are very expensive and this may unfortunately prevent the microscopist from having convenient access to the most appropriate type of microscope.

Microscopy is an extremely broad scientific discipline, involving a wide variety of microscopes, techniques, and materials. Scientists and engineers in almost every discipline (biology, materials science, chemistry, geology, physics, environmental, mechanical, electrical engineering) and also in their subdisciplines (histology, cytology, metallography, mineralogy, pathology) utilize microscopes. Microscopes are used routinely in forensic, industrial, environmental and hospital laboratories to characterize, compare and identify a wide variety of substances (eg, protozoa, bacteria, viruses, plant and animal tissue, rocks and minerals, wood, ceramics, metals, abrasives, pigments, foods, drugs, explosives, fibers, hairs) and even single atoms. Microscopists also do basic research in instrumentation design, specimen preparation techniques, and new applications of microscopy. These applications include forensic trace evidence, contamination analysis, art conservation and authentication, asbestos control, air quality assessment, and many others. In addition, microscopists help to solve production and process problems, control quality, handle general troubleshooting problems, and customer complaints. Many industries have integrated optical, electron, and scanning probe microscopes into their computer controlled inspection lines. Given the trend in device miniaturization, few industries and academic institutions can now function adequately without utilizing some form of microscopy.

To keep microscopists informed of ongoing advancements in microscope hardware, software, and technique, there are numerous scientific journals and professional societies devoted exclusively to microscopy (1). A microscopy review article is featured every 2 years in *Analytical Chemistry* (2) and an ever increasing wealth of information concerning microscopy is available on the internet. Customer demand continues to guide microscope manufacturers to improve their microscopes along the lines listed in Table 2

2. Optical Microscopy

2.1. History. Microscopy as a field follows only astronomy in the history of science and technology. In 1630, Stelluti published the oldest known

microscopical observations, which were on the microstructure of the bee and the weevil. The compound optical microscope is based on a two-lens, two-step magnification by objective and ocular, and was proposed by Zacharias Jansen in 1590. However, because of the difficulties associated with machining lenses that were free of spherical and chromatic aberrations, as well as other faults of the early compound microscope, most microscopists preferred the simple one-lens magnifying glass for the next 200 years. Even so, Antoni van Leeuwenhoek (1632–1723) in the late seventeenth and early eighteenth centuries developed simple lenses capable of magnifications nearly as high as 300×. The resolution was adequate for the detection and identification of blood cells, spermatozoa, and even bacteria, all reported by Leeuwenhoek in a long succession of letters to the Royal Society in London. Robert Hooke (1635–1703) made similar studies in England, principally on biological materials.

The development of corrected (achromatic) lenses and the addition of polarizing Nicol prisms, both ~1830, marked the real beginning of light microscopy. The most important applications then followed rapidly. For example, toxicology applications, involving microchemical reactions for arsenic, lead and mercury, and forensic applications to blood, hair, and fibers. During the period 1850–1900, optical crystallography, mineralogy, and metallography developed into recognized fields of study. Many of these developments were the work of Henry Sorby (1826–1908), who also first fitted a spectroscope onto a microscope to better characterize and identify colored substances (eg, blood, dyes, and pigments). Others, including Otto Lehmann during the late 1800s, added a heating stage to the polarized light microscope (PLM) and developed phase and composition diagrams, as well as, studying liquid crystals.

By 1900, Emile Chamot (1866–1950) at Cornell University was teaching optical microscopy courses in water, food, and microchemistry. Chamot's most significant contribution was the development of microchemical procedures with his first volume on chemical microscopy appearing in 1916 and the most recent edition in 1983 (3). During the same period, Simon Gage, also at Cornell, was actively developing the biological applications of the light microscope (4). The combined works of these two teachers served as the foundation for the development and application of microscopy in the world of science and technology during the first one-half of the twentieth century. However, many other microscopists including Hartshorne and Allen, also contributed greatly to spreading the use and furthering the development of microscopy (5,6).

The microscopes used by chemists, biologists, and materials scientists during the nineteenth and early twentieth centuries were essentially identical, differing principally in the presence of polarizing filters (ie, an analyzer and polarizer) and a rotating stage on the petrographic or materials science microscope. Since that time, there have been many advancements and modifications to the basic light microscope, many of which are discussed below. These include accessory attachments that provide increased resolution or contrast, or new types of image signals. Entirely new types of light microscopes have also been created. Some utilize a scanned beam of light (eg, scanning optical microscope, SOM) instead of a fully illuminated field as in a conventional light microscope, others utilize (uv, ir), or Raman scattered light to create an image. These new types of microscopes, which incorporate high resolution digital imaging systems,

spectrometers, and the most advanced optical components, are currently the most active area of research and development.

2.2. Microscope Components and Their Functions. The components of a transmitted polarized light microscope (PLM) are shown in Figure 1. The PLM is essentially the same as a standard brightfield microscope used for biologic applications except for the presence of the polarizer, analyzer, compensator slot, Bertrand lens, and rotating stage. On most microscopes, the illumination is provided by an intense (eg, 100 W) quartz halogen bulb, usually housed within the base or rear of the microscope. Specialized bulbs (eg, Hg-vapor, C-arc, cesium) are often used to emit a specific spectrum of wavelengths. Lasers are also used if highly monochromatic uv, visible, or ir light is desired. Ultraviolet light sources are usually used to excite fluorescence in stained or natural biologic specimens, minerals, or semiconductors although they may also be used to provide higher spatial resolution. As the light exits the base of the microscope its diameter may be reduced by a field diaphragm. In a properly aligned microscope (ie, Köhler illumination), the field diaphragm will be used to reduce excess glare. The light then passes through a polarizing filter called, the "polarizer". The function of the polarizer is to produce plane-polarized light (PPL), ie, light in which all of the rays vibrate in a single plane. The orientation of this plane is controlled by the position of the polar's privileged direction, which is oriented east–west in all modern PLMs. Next, the east–west polarized light passes through the aperture (or iris) diaphragm, which has the following effects when its diameter is reduced, or "stopped down": (*1*) the light intensity is reduced without changing the color temperature; (*2*) the degree of contrast within the sample is increased and; (*3*) the depth of field is increased. Since these results are accomplished by reducing the diameter of the light, the numerical aperture is also reduced, this causes a decrease in the spatial resolution (7,8). The light then impacts the convex surface of the substage condensing lens. The condensing lens causes the light rays to be refracted toward a central area, thus increasing the light intensity. By mounting the condenser on its own vertically adjustable rack, the area of most focused illumination can be precisely positioned at the imaging plane of the specimen. This attention to optical alignment will result in images of higher brightness, contrast, and resolution. The light then passes through an opening on the stage and through the sample. Microscope stages come in two basic types: circular, rotatable stages and rectangular, mechanically translatable stages. A circular stage is almost always present on a PLM and it may also be fitted with a mechanical or electronic translation stage. After the light interacts with the sample, it passes into the objective lens. The functions of the objective are to collect the light exiting the sample and to produce an enlarged, intermediate image. The light gathering ability of a lens is called the numerical aperture and is proportional to the size of the cone of light that enters the objective. Objectives are available in a wide range of magnifications ($0.5\times$–$250\times$), numerical apertures (0.1–1.5) and degrees of perfection (eg, absence of spherical and chromatic aberrations). Specialized objectives are available for uv or ir transmission, long working distance, fluid immersion applications, and reflected light microscopy to name a few. Objectives are commonly threaded into a rotatable turret so that changing magnification is convenient. The next three microscope components, the analyzer, compensator slot, and Bertrand lens are only present on PLMs

and must be inserted into the light path to be utilized. The analyzer is identical to the polarizer except it is rotated 90° so that its privileged direction (ie, the direction that permits light to pass) is oriented perpendicular to the lower polarizer (ie, north–south). When the analyzer is inserted, observations are said to be viewed in "crossed-polarized light" (XPL), whereas if the analyzer is retracted observations are in PPL. Note that the mutually perpendicular orientations of the privileged directions of the polars would result in a completely black field of view if no sample was present, or if the sample was optically isotropic (ie, amorphous or isometric, see the discussion of PLM below). The compensator slot allows for the insertion of various specialized crystal plates of known optical properties. These properties are superimposed with those of the sample in XPL observations and allow the determination of several diagnostic properties of the sample (eg, optic sign, sign of elongation, refractive indexes, elliptical polarization) and also may be used to increase sample contrast. The next component, the Bertrand lens, is used with crossed polars to view an interference pattern or "figure" formed at the objective back focal plane. Only crystalline materials possessing more than one index of refraction can produce an interference figure. Interference figures are used to determine the optic sign and symmetry of a crystal. The Bertrand lens may also be used to assist in aligning the optical and illuminating systems of the microscope. Observations made using the Bertrand lens are termed "conoscopic" whereas normal observations are "orthoscopic". The eyepieces or oculars are the final component of the microscope and serve to magnify the intermediate image formed by the objective, however, eyepieces do not increase resolution. The best eyepieces have a wide field of view (eg, >23 mm), are focusable and have a high eyepoint (ie, the distance required between the eye and lens for comfortable viewing of the image). Microscopes intended for photomicrography will have an additional overhead view port for mounting a camera.

Microscope designs may vary significantly from that of Figure 1, depending on the application. For example, metallographers and biologists often prefer an "inverted" microscope design as opposed to the standard "upright". In an inverted microscope the position of the objectives and illuminating system (ie, bulb, condenser) are switched and the sample is placed up-side-down on the stage. Microscopes may also be equipped to provide vertical or "reflected" light illumination, whereby the illumination is passed through the objective and onto the sample. Reflected light is required for viewing opaque samples (eg, metals, minerals, semiconductors) and may also be useful when viewing transparent samples, in particular surface features.

There is also a wide selection of optional components for the compound microscope. Each of these components was devised with the goal of either, increasing resolution (vertical or lateral), increasing sample contrast, or providing new types of characterization data. Some of these optional components are only appropriate for certain samples, whereas others are beneficial to all types of samples. Optional components vary in complexity from simple color balance correction filters to complete redesigns of the microscopes systems (eg, illumination, magnification, detection), as in a laser scanning confocal microscope (LSCM). The LSCM is a type of SOM that is significantly different from a conventional microscope. In a SOM, a focused spot of light is scanned over the field of view (ie, point-source illumination) instead of illuminating the entire field of

view all at once as in full-field illumination. Thus, at any given instant only a single spot of the sample is illuminated (Fig. 2). During the time this spot is illuminated, a spectrometer or other detector (eg, digital camera) may record the intensity or wavelengths (eg, color or spectrum) emitted or absorbed at that particular spot. Thus, a complete image is formed only after the beam has scanned the entire region of interest.

2.3. Optical Resolution and Contrast. The resolution of the best microscope of the early nineteenth century was only slightly less than that of present-day microscopes (~220 nm). The two most important improvements that allowed light microscopes to achieve close to their theoretical resolution were (*1*) the principles of proper alignment for the illuminating and optical systems set forth by August Köhler (9) and, (*2*) the invention of "apochromatic" objectives by Ernst Abbe (8). In 1888, Ernst Abbe, presented his diffraction theory of resolution for the light microscope (7). This theory made it possible for microscopists to understand and use the microscope as a high resolution instrument. Abbe's equation states that resolution (R) improves with higher numerical apertures (NA) and shorter wavelengths ($\bullet$).

$$RP = 0.61\ \lambda/\mathrm{NA} \tag{1}$$

In Equation 1, the Rayleigh constant 0.61 is related to the detectability of resolution and $\bullet$ is in nanometers ($1\ \mathrm{nm} = 10^{-9}\ \mathrm{m}$). Resolution is defined as the minimum distance between two adjacent points such that both points are seen as distinct objects. The numerical aperture is the measure of the light gathering ability of a lens (eq. 2).

$$\mathrm{NA} = n\ \sin\ \mathrm{AA}/2 \tag{2}$$

In equation 2, n is the refractive index (n) of the medium between the objective and coverslip and AA is the average angular aperture of the objective and condenser. Attempts have been made to increase resolution by using higher refractive index objective lenses (even diamond), however, so far the difficulties have outweighed the advantages. Table 3 shows the effects of NA on resolution for a range of objectives at wavelengths of 550 and 200 nm. These wavelengths were selected for two reasons: (*1*) 550 nm (ie, green) is close to the average wavelength of white light and is a wavelength where the human eye is very sensitive, and (*2*) 200 nm is close to the shortest wavelength of laser light employed in a high resolution LSCM. Table 3 shows that the highest resolution achieved in air, and using white light, is 355 nm. The use of uv light and a higher NA immersion objective can result in a resolution of up to ~90 nm. However, note that the depth of field (DOF) decreases rapidly with increasing NA. High NA, low DOF objectives are purposefully used in confocal microscopes to achieve better vertical resolution (ie, thinner optical slices). Also note that the use of uv light requires that uv-transparent quartz optics or reflection optics be utilized rather than standard transmission optics. Ultraviolet light also requires that the images be recorded by camera since the human eye cannot detect and is damaged by uv light.

As previously mentioned, the contrast exhibited by a specimen may be increased by reducing the angular aperture using the aperture diaphragm, however, this decreases the resolution of the image. The contrast exhibited by a sample may also be greatly increased by mounting the sample in an appropriate media (eg, water, refractive index oil, epoxy, etc). This simple practice may obviate the need for any new instrumental technique for enhancing contrast. According to the laws of refraction, when a particle is mounted in a medium having a matching refractive index, the particle will lose contrast and appear to disappear completely. Conversely, the particle's contrast will increase rapidly as the difference in refractive index increases. Therefore, if the sample is suitable for mounting in a liquid, then the first step is to select a liquid with the most appropriate index. Unfortunately, biologists are often restricted by their specimens in their choice of mounting media. Water ($n_D = 1.33$) is far superior to glycerol ($n_D = 1.47$) or Canada balsam ($n_D = 1.54 \pm 0.01$) for most biological substances whose refractive indexes lie in a narrow range near 1.54. Other methods for improving specimen contrast utilize specialized illumination systems or beam splitters that are incorporated into the design of the microscope. Several of the most common and useful contrast-enhancing accessories are discussed below. An excellent discussion of the standard methods of improving contrast up to the digital age is available (10).

2.4. Specialized Techniques for Improving Contrast and Resolution. *Polarized Light Microscopy.* The use of polarized light to measure diagnostic material properties was one of the earliest improvements to the compound optical microscope, dating back to the 1830s. This improvement involved the placement of Nicol prisms on either side of the sample and the use of a rotating stage (11). Developments in PLM have continued to date with the most advanced and quantitative PLMs now utilizing liquid-crystal polarizers (12). The basic principles of imaging with polarized light are given in Figure 3. When plane-polarized light is transmitted (or reflected) into an anisotropic material (ie, a material exhibiting birefringence) the light ray is split into two rays. Each ray remains plane polarized, but the vibration directions of the two rays are perpendicular to each other. Since the material transmitting the light is birefringent, the two rays will not travel at the same speed. The ray traveling in the direction of the material's lower refractive index will be faster and thus will exit the material ahead of the slower ray. This difference in velocity causes a path difference (also called retardation, denoted Δ) to develop between the two rays and is demonstrated in Figure 3 by noting that when the light enters the crystal (at position 1) the fast and slow ray are in-phase, but after both rays pass through the crystal, the fast ray (in orange) is ahead of the slow ray (in green) by a distance of approximately one wavelength. The method by which this path difference is transformed into a visual observation is shown in the upper portion of Figure 3. As the fast and slow rays travel through the analyzer, only the component of each ray that can be resolved into the north–south privileged direction of the analyzer is passed. As these portions of the slow and fast rays are once again resolved to vibrate in the same plane, their interference produces a new color, or in the case of monochromatic light, a different intensity of the same color. Depending on the thickness and birefringence of the crystal, the interference may vary from constructive to destructive. The interference color seen at each location

on the sample represents of the magnitude of the retardation and may be quantified using the Michel Lévy interference color chart or a calibrated digital camera (Fig. 4). A more in depth discussion of the interaction of polarized light with matter is beyond the scope of this article. Many excellent textbooks are available on the practical and theoretical aspects of the use of the PLM (13,14).

When ordinary white light is used to illuminate a sample (as is typical), a multitude of optical observations and measurements may be performed using PPL or using XPL. With PPL it is common to measure such properties as refractive indexes and pleochroism, ie, the ability of a material to selectively absorb certain wavelengths. By using XPL, such properties as: twinning; birefringence; dispersion data (ie, the variation in refractive index with wavelength), extinction phenomena; and many other properties may be measured. Accessory plates or "compensators" containing crystals of known optical properties may also be inserted into the light path to assist in measuring such properties as the optic sign and sign of elongation. Another standard accessory, the Bertrand lens, may be used to determine the optic orientation of the grain, its 2V or its crystal system.

When all of the possible measurements made using polarized light are combined with other readily available physical and chemical characterization data (eg, color, reflectivity, size, morphology, microstructure, defects, solubility, melting point, etc), a large set of highly diagnostic data is available on a single sample that may be as small as 500 nm. A microscopist can usually collect a greater quantity of physical and chemical characterization data in less time using a PLM than with other more expensive and more sample restrictive microscopes (eg, SEM, SPM). However, the measurement of optical properties is not always the goal of the microscopist, so the PLM is certainly not the most appropriate type of microscope for all samples. The PLM is best suited for rapid identification of particles down to ~500 nm. With the proper training and experience it is not uncommon for a light microscopist to have instantaneous sight recognition for hundreds of substances. This skill is particularly useful in forensic work and in contaminant-identification, where a diverse assemblage of particles such as spores, natural fibers (eg, cotton, animal hair), metal flakes, mineral grains, explosives, drugs, food, paint, synthetic fibers (eg, rayon, polyester), skin cells, etc, may be present in the same sample. The same efficiency for identifying particles would not be possible using other types of microscopes.

Another significant capability of the PLM is its ability to differentiate between polymorphs, ie, different crystallographic forms of the same chemical substance. For example, the three forms of titanium dioxide (brookite, rutile, anatase); the three forms of calcium carbonate (calcite, aragonite, vaterite); the four forms of the high explosive HMX. Polymorph identification is an important application of PLM because the properties exhibited by different polymorphs may be quite different. In fact, the PLM is the only instrument mandated by the U.S. Environmental Protection Agency (EPA) for the detection and identification of the six regulated forms of asbestos and other fibers in bulk samples.

An important polarized light technique known as dispersion staining (15) was introduced during the 1940s by Germain Crossmon (7,8). This technique utilizes a special objective that contains either a central or annular opaque stop (Fig. 5). The dispersion staining technique exploits the interaction of

the dispersion properties of the mounting media and the sample to cause the sample to appear to have "stained" edges (Fig 5). When performing dispersion staining, the best results are obtained when the dispersion curves (ie, wavelength vs refractive index) of the mounting media and the sample intersect steeply in the visible light region (Fig. 5). As white light passes through the crystal, the wavelength (ie, color) for which the refractive index of the liquid and the solid match ($\bullet_0$) will not undergo refraction. This wavelength (eg, blue) will travel axially through the objective and will be absorbed by the opaque stop. The opaque stop together with the aperture diaphragm will also remove nearly all of the white light that passed undeviated through the mounting media and the particle's interior, thereby causing the mounting media and the central areas of the grains to appear dark. The remaining portion of white light that is refracted at the grain boundary enters the objective at such an angle that it passes around the perimeter of the stop and is transmitted to the eyepiece for viewing. However, recall that in this example the blue component has been removed from this refracted white light. Thus the perceived color is yellow, the compliment of blue. If an annular stop were used instead of a central stop, then the edges would have a blue color and the background would be white. Since the central stop technique provides greater contrast it is more often employed. Note that when performing dispersion staining on a birefringent material in polarized light the dispersion staining colors will vary depending on the grain's crystallographic orientation.

A typical application is the identification of asbestos in bulk building materials. It is also used in forensic laboratories for the rapid identification of drugs, explosives, fibers, and minerals. It is also often applied to the "needle-in-a-haystack" detection of any particular substance in a mixture, such as chrysotile in insulation, cocaine in dust samples, quartz in mine samples, or any particular mineral of interest (eg, tourmaline) in a forensic soil sample.

Darkfield Illumination. Darkfield illumination is a technique in which the illumination is directed obliquely at the sample using either transmitted or reflected light. This arrangement was developed for providing enhanced contrast of biological specimens because, as stated previously, the refractive index of biological material ($n \sim 1.54$) and that of the desired mounting medium may be very similar, resulting in low contrast. In darkfield illumination, an opaque disk or "stop" is placed directly below the condenser (Fig. 6). The size of the stop is such that only the light along the perimeter of the stop passes into the darkfield condenser. The resulting illumination has a 3D shape resembling the surface of a cone. When a specimen is present, the obliquely directed rays strike the sample and where suitable conditions occur, a portion of the light is reflected, refracted and/or diffracted into the objective lens. In the areas adjacent to the sample, occupied only by mounting media, the oblique rays pass unscattered to locations outside of the field of view. Thus, regions of the sample where light is not scattered into the objective will appear dark. A greater degree of contrast and sometimes a more 3D appearance result from the darkfield image being free of the unscattered light component (16). In fact, details much smaller than the resolving power of the microscope are visible, although they are not fully resolved. For example, asbestos fibrils commonly present in floor tile or air samples as 20-nm fibers are made visible, although they are by no means resolved. Other

samples amenable to darkfield are living microorganisms, insects, colloids, minerals, ceramics, polymers and any thin sections containing imperfections or gradients in refractive index. Darkfield is not usually appropriate for thick samples and can create an unnatural appearing image, especially if the optical system is not precisely aligned.

For those interested in creating their own darkfield microscope, an opaque stop (7–15 mm in diameter, depending on the objective used) can be taped to the bottom of the substage condenser of a standard light microscope. This stop will create a cone of illumination that will be sufficient to achieve good darkfield images for some samples.

Phase Contrast. In 1934, Fritz Zernike introduced the technique of phase contrast. This technique was immediately seen as an improvement over darkfield (10,17). Like darkfield illumination, phase contrast employs a hollow illuminating cone, but the cone is within the objective aperture rather than outside of it, as in darkfield. The hollow cone of light is created by a transparent annulus in an otherwise opaque stop located in the substage condenser. This hollow cone of light interacts with details of the specimen to yield both zero-order and higher order diffraction rays. In the hollow cone, the zero-order rays all pass into the objective and then through a phase ring. The phase ring is conjugate to the phase annulus in the substage condenser. The higher order diffracted rays (which are now out of phase by 1/4• relative to the zero-order rays) deviate from some of the other diffracted rays into the dark cone and through the phase plate, but not through the phase ring. The optical path difference between the direct rays passing through the phase ring and the diffracted rays passing through other areas of the phase plate introduce an additional 1/4• path difference (and therefore a phase difference) between the direct zero-order rays and the diffracted first and higher order rays from the same object detail in the specimen. Upon recombination in the microscope image, destructive interference occurs for those rays one-half wavelength out of phase and thus greatly improves the contrast. Because the phase condenser annulus lies in the outer region of the condenser aperture, the resulting oblique rays provide full resolving power, corresponding to a fully open substage aperture diaphragm.

Phase contrast may be performed in transmitted or reflected light and is most useful to the biologist who often needs to differentiate between biological entities (eg, plants, cells, spores, pollen, diatoms), most of which have similar refractive indexes and little if any birefringence. Phase contrast optics are also useful because they increase the sensitivity of refractive index determinations using the Becke line method. Polymer characterization may also be greatly assisted, especially for emulsions and multilayer polymer films that exhibit gradients in refractive index.

Differential Interference Contrast. In 1950, differential interference contrast (DIC) was invented by Georges Nomarski (10,18). Soon after its invention, it became clear that for most samples DIC provided a level of contrast that was superior to that achieved with other techniques. Furthermore, DIC utilizes polarized light and can be performed on a wide variety of materials in either transmitted or reflected light. Like phase contrast, DIC relies on interference, however, the separation of a given beam and its subsequent recombination after interaction with the sample is accomplished quite differently. Nomarski

used the double refraction (ie, birefringence) of a calcite crystal (actually a Nomarski-modified Wollaston prism) to split the incident light into fast and slow rays (Fig. 7). After these rays emerge from the calcite crystal, they have a separation distance (ie, path difference or retardation) proportional to the thickness of that crystal, but purposely less than the resolution of the objective to be used. For this reason, a separate Nomarski prism must be utilized for each objective. When DIC is utilized with transmitted light, the two rays traverse different optical path lengths in the object space as, eg, one ray passing through the edge of an object and the paired ray passing through the adjacent mounting medium. This produces a phase difference between the two rays and on recombination in a second Wollaston prism, interference contrast results.

When DIC is employed with reflected (ie, vertically incident) light the upper Nomarski prism serves as both the beam splitter and recombiner. Reflected light DIC is an extremely effective technique for enhancing the contrast of surface microtopography (eg, steps, growth spirals, etch pits, cracks, etc). The level of contrast obtained is often quite stunning (Fig. 8). Topographic offsets of <10 nm can be easily resolved. The relative heights of surface features may be quantified to the extent that the interference colors can be measured. Given the high surface sensitivity of DIC, this would be an excellent technique to incorporate on a scanning probe microscope.

Unfortunately, DIC images are in a sense, sheared images. The two rays from the lower prism lie in a specific vertical plane. This causes the DIC effect to vary depending on the orientation of the crystal. The greatest degree of contrast will be observed for crystal orientations exhibiting the highest birefringence. There will be no contrast effect perpendicular to the plane of the two illuminating ray directions. This orientation dependence of the contrast can be compensated for by simply rotating the crystal on the stage and/or by partially rotating the analyzer. Still, there is an advantage to the shearing method. In addition to a 3D effect, the contrast effects observed in the shearing plane identify the higher and lower index areas. This furnishes an excellent way of comparing refractive indexes, eg, in glass samples recovered in a crime lab hit-and-run case. If such a glass particle were mounted in an appropriate refractive index liquid and heated using a microscope hotstage, the particle would disappear at the temperature where the index of the mounting medium and particle matched. With DIC, the contrast effect at the particle boundary will reverse at that specific temperature from light-to-dark, to dark-to-light across the boundary of the particle.

Since DIC is an interference method that utilizes polarized light, interference colors are produced. This means that one can estimate the retardation of a given particle relative to that of light passing through the adjacent medium. The pattern of retardation presented in the DIC image reveals at a glance whether a given particle has an index higher or lower than the medium. This makes DIC a useful method for the mineralogist or forensic scientist for examining mineral grains. Reflected light DIC is useful for examining surface defects, anisotropies, and roughness in metals and semiconductors. DIC is used widely in the biological sciences for enhancing the structural details of plant and animal tissue.

Fluorescence Microscopy. A fluorescence microscope is essentially the same as a conventional microscope except that the light source emits low

wavelength (high energy) uv light. Ultra-violet transmitting quartz optics and a variety of filters (high pass, low pass, band pass) may be placed above and below the sample to select the wavelengths of the illuminating (ie, stimulating) and collected (ie, perceived) light. The most advanced type of fluorescence microscope is the laser scanning confocal microscope (LSCM) (see also CONFOCAL MICROSCOPY SECTION). When a fluorescent sample is exposed to uv light, electrons in ground states (eg, valance band) will be excited into higher orbitals. This excitation produces a vacancy or "hole" in the valance band and causes an electron from a higher energy level to cascade down to fill this hole. As this electronic transition from high to low energy takes place, a surplus of energy is released in the form of a visible photon (19). With the appropriate long or band pass filters in place, only the fluorescent wavelengths will be transmitted or reflected to the eyepieces or camera. Since fluorescence is often the result of elements present in trace amounts [eg, parts per million (ppm)] rather than bulk quantities, it is often useful in the crime laboratory for the comparison of materials collected from suspect and crime scene. The excitation wavelength, color, intensity, and distribution of fluorescence may be diagnostic qualities of the material. Particles of the same substance from different sources almost certainly show a different group of trace elements. Fluorescence is an effective and nondestructive means for authenticating natural and synthetic gems and precious stones and semiconducting materials. The most widespread use of fluorescence microscopy, however, is in the biological sciences (eg, medicine, molecular biology, plant physiology, etc). A countless number of fluorescent "labels" or "tags" exist, which bind preferentially to specific proteins, antibodies, receptors, bone, viruses, microbes, etc. These labels allow the spatial distribution of biological substances or parts there of to be directly visualized, oftentimes as dynamic life processes or chemical reactions, are occurring (20).

Confocal Microscopy. The main feature of confocal microscopy is that only the in-focus rays are used to form the image. This results in improved contrast and a distinct improvement in resolution (10,17). To achieve these results, significant modifications and additions are made to nearly all of the microscope's subsystems (eg, the illuminator, lens, detection system). Image collection in the confocal microscope is fundamentally different from that of a conventional light microscope (Fig. 2). In a LSCM, a point source of monochromatic laser light is rastered over the area of interest and the light intensity at each position is recorded by a detector. The use of dichroic mirrors and other filters (high, low, and band pass) allow the user to select the detected wavelengths. As the beam is scanned across the sample, successive points are plotted to form a complete image. Thus, at no moment in time is there an actual image of the sample formed in the microscope, only a point of light interacting with the sample and a flux of light emanating from that point.

A second design of confocal microscope is the tandem scanning microscope (TSM). The TSM utilizes a Nipkow disk that contains thousands of tiny apertures arranged in an Archimedes spiral near the outer edge. These apertures are used to create and project thousands of very narrow light rays to a plane within the specimen. Each of these rays lies on the surface of the hollow cone that illuminates the object. A second Nipkow disk, which is conjugate with the first disk, rotates in exact synchronicity so that each of the focused rays of

light may be transmitted to a viewing screen. Again, all out-of-focus detail in the specimen is not illuminated and hence not visible. The absence of the fuzzy, out-of-focus portion of the image leaves a sharp, high contrast, well-resolved, in-focus image.

LSCMs are commonly equipped to provide fluorescence microscopy capabilities. This is a good combination of techniques because the laser light is highly monochromatic and therefore can be more easily filtered out of the image than less monochromatic light. In addition, the confocal aperture allows the highest lateral and vertical resolution possible in any optical microscope and allows depth profiles or "optical sections" and 3D reconstructions of bulk samples. The ability to carefully adjust the position, diameter, intensity, and dwell time of the light is particulary of great advantage to fluorescence methods. This reduces the negative effects associated with conventional full-field fluorescence detection, such as photobleaching, low signal-to noise ratio and lower spatial resolution. LSCMs may also be used with polarized white light sources to produce all of the characterization data of a PLM. When the LSCM is used with an ir laser, ordinarily opaque samples such as semiconductors may be transparent. LSCM has many applications in the semiconductor industry since it is nondestructive and it capable of providing physical and electronic structure information (eg, band gap, binding energies, molecular orientation, defects) (21).

Cathodoluminescence Microscopy. A cathodoluminescence microscope attachment provides an electron beam built into the stage of a PLM (22,23). The impact of high energy electrons causes the release of characteristic X-rays and on some samples visible fluorescence (ie, luminescence). The energies of the X-rays can be measured with an energy dispersive spectrometer (EDS) and the distribution of the fluorescence can be observed through the microscope or with a camera. When exhibited, luminescence provides useful documentation for the distribution of trace elements that are usually below the detection limit of EDS. Such an instrument combining EDS and PLM provides essentially the same information as an electron probe microanalyzer (EPMA). Cathodoluminescence detectors are oftentimes found on SEMs or EPMAs.

Microspectrometers. Microspectrometer is the general term for an instrument that collects spectroscopic information from a microsized location. This is accomplished by utilizing the magnification and light condensing systems of a microscope to focus an intense beam of light at a particular location. The light is collected by the objective and its intensity and wavelength are measured by a spectrometer or suitable detector. Although a microscope is employed, in general microspectrometers do not provide an image, but only provide a spectrum from a microscopic location. Recognizing this, microspectroscopic techniques are sometimes referred to as microprobes. However, the nomenclature can be somewhat cryptic and a given instrument, eg, the Raman microprobe, may also be known as the laser Raman microscope, micro-Raman spectroscope, or the molecular orbital laser examiner (MOLE).

A growing number of microspectrometers are now available that do provide good spectroscopic images in a reasonable time. Older instruments could require many hours or an entire day to record a single image. Modern instruments may require only a few seconds, but several hours would not be uncommon for a high resolution image. A major improvement to imaging has been the use of detectors

that posses an array of light sensors (eg, 10×10). Although this type of sensor produces an image containing only 100 data points (ie, pixels), image resolution and field of view may be increased by combining adjacent areas. When utilizing an array detector, the light beam is not scanned but the image is projected directly onto the elements of the detector. Traditional single-sensor detectors do, however, utilize a scanned beam of light like any other SOM, and the light intensity and wavelength are measured at each point on the sample.

Images may be collected using two levels of detail. In the simpler and faster method the spectrometer is set to detect light of only a particular wavelength. The contrast (ie, grayscale) in the image shows the spatial distribution of the light intensity for that wavelength. In the second method, the spectrometer collects a spectrum at each point on the sample. In this method, once the image has been collected the data can be adjusted or mathematically manipulated so that the image can be presented in a variety of different ways. Although the second method provides much more characterization data, it is used less often because image acquisition is often very time consuming. With recent technological advancements there has been a general trend for single point microspectroscopic techniques (ie, microprobes) to be extended to provide microscopic imaging capabilities.

As spectroscopy is a field as broad as microscopy, this article will only briefly discuss the two most common types of imaging microspectrometers. These are the Raman microscope and the ir microspectroscope.

Raman Microprobe. When monochromatic laser light interacts with a material, the majority of it is elastically scattered as light rays of the same wavelength (ie, color), this is the Raleigh scattered component (24,25). However, a very small component ($\sim$1 in 10^7 photons) of the incident light is inelastically scattered at different wavelengths, this is the Raman scattered component. The difference in energy between the incident light (known) and the Raman scattered light (measured) is called the Raman shift. Raman shifts result from the fact that some of the incident light energy is used to change the vibrational, rotational, or energetic state of the material. Raman scattered light may be of a lower energy (Stokes scatter) and higher energy (anti-Stokes scatter) than the incident beam, although the frequencies are not different. The anti-Stokes (higher energy) scatter is possible because some of the molecules in the sample may be initially in an excited state. However, since the population of these exited states is usually far less than ground states, the anti-Stokes signal is usually weak. Nonetheless, this signal can be very informative. Interestingly, the ratio of the Stokes to anti-Stokes intensity is proportional to the sample's temperature.

Since no two materials have identical molecular structures, the Raman spectrum is regarded as a fingerprint for a material. Apart from using Raman spectra for absolute identification, spectra are also used to test theories on crystal and molecular structure, provide quantification of material properties, and measure concentrations. Because Raman spectra can be obtained on almost any material and in any state (solid, liquid, gas), there are applications in a wide range of fields. Some examples include: polymer chemistry, mineralogy, ceramics, semiconductor defect analysis, forensic science, medicine, and *in situ* studies of chemical reactions. Samples may be analyzed with little or no preparation and detailed *in situ* and real-time studies may be performed with materials

placed in reaction chambers held under conditions of controlled temperature, pressure, or atmosphere. Samples may also be adsorbed to a metal surface (eg, Ag, Cu, or Au). This practice results in an enhancement of the Raman scatter by as much as 10^6 times, by a process known as surface-enhanced Raman scattering (SERS). SERS typically provides detection in the monolayer range. In general, Raman is more sensitive than Fourier transform infrared spectroscopy (FTir) and has a smaller sampling (ie, interaction) volume of $<1\ \mu m^3$, ($<0.01\ \mu m^3$ for SERS) compared to $\sim 50\ \mu m^3$ for FTir. For increased resolution and sensitivity, a confocal Raman system may also be constructed.

Infrared Microspectroscopy. In an ir microspectroscope or FTir microscope, ir light is either transmitted through or reflected from a sample and the absorbance, transmittance, or reflectance is measured (26). The wavelength of the light employed is typically in the range of 2.5–25 μm, which is equivalent to a frequency (in wavenumbers) of 400–4000 cm^{-1}. When ir light penetrates a substance, a fraction of the light's energy causes the molecules or bonds within that substance to undergo characteristic motions, such as vibration, rotation, bending, and stretching. The frequencies at which a material exhibits these motions is diagnostic of the types of molecule(s) or bond(s) present within that material. For example, stretching of the O–H bond in an alcohol results from absorption in the range of 3400–3100 cm^{-1}. The ir absorption is extremely useful for the identification of organic functional groups (eg, amine, alkane, alkene, alkyne, aromatic) and bonds within inorganic compounds and minerals (eg, sulfate, carbonate, water). The ir spectra may be obtained on any material that contains a molecular asymmetry. However, the lack of an ir spectrum may also be an important quality.

Many substances that are opaque or semiopaque using visible light may be transparent in the near ir (eg, silicon, iodine, potassium permanganate). In some ir microspectroscopes an ir camera similar to that used in night vision applications is used to collect an image of the sample. Most instruments also operate with visible light to conveniently view the sample and select the area to be analyzed. Images can also be obtained by collecting spectra or intensity data at many points on the sample and plotting a grayscale image. Such images are useful for identifying internal defects or impurities.

Computer-Assisted Contrast. Software can provide an extremely convenient and oftentimes inexpensive means for enhancing contrast. In state-of-the-art systems, a computer is directly interfaced with a digital camera that is attached to a microscope and digital contrast enhancements can be performed simultaneous with image collection. Alternatively, and with nearly the same effectiveness, digital images can be enhanced after they have been collected using image analysis or photoenhancement software packages (27). Although software cannot increase the resolution of the collected image, it is common that a simple adjustment to the brightness, contrast, intensity, hue, or color saturation is adequate to bring out unseen image details. In addition, the resulting images can be of both high contrast and high resolution because they may be collected with a fully open substage aperture (a setting that typically shows low visual contrast). More advanced image processing filters or "kernels" may be applied systematically to groups of adjacent pixels. These filters may allow the removal of random noise (eg, low pass), the subtraction or addition of two images,

and image differentiation, to name but a few kernels. The increasing role of computers in image collection and processing has been progressive since the 1970s, when video processing was state-of-the-art. As Shinya Inoué, author of a classic text in the field, states: "We can now see objects that are far too thin to be resolved, and extract clear images from scenes that appeared too fuzzy, too pale, or too dim, or that appeared to be nothing but noise" (28).

Advanced image processing software is now being used to increase the depth of field in otherwise mostly out-of-focus optical images. This is accomplished by collecting a series of images each taken at a slightly different focus and then digitally combining only the in focus regions from each of the images. This technique also provides an x, y, z coordinate for each pixel in the image, thus allowing quantitative 3D measurements and reconstruction or renderings. This technique provides optical sectioning capabilities similar to that of a confocal microscope except that the spatial resolution is not enhanced. Image analysis software is also useful for automatically tracking moving subjects and counting particles based on size, color, shape, or other optical properties.

3. Electron Microscopy

3.1. History. During the nineteenth and early twentieth century, it was realized that there was a need for a microscope with greater resolution than the optical microscope. As it was known that the very short wavelengths of electrons could theoretically provide subnanometer resolution, work was begun on the first electron microscope. After a sustained research effort toward this need, Ernst Ruska developed the first TEM ~1931. This was the first microscope to exceed the 500-nm resolution limit, of the best optical microscope of the time. By 1938, von Ardenne had improved the TEM resolution to between 50 and 100 nm (29). Simultaneous with the development of the TEM, pioneering research at the RCA Laboratories by Zworykin, Hiller, and Snyder led to the construction of the first SEM in 1942 (30). Although this SEM initially achieved a resolution of only 1000 nm, subsequent improvements increased the resolution to 50 nm. However, this was still less than the resolution of the TEM available at that time.

During the period from 1948 to 1965, research in SEM design led by C. W. Oatley at the University of Cambridge greatly improved on the SEM of Zworykin. Significant improvements were made to the design of electron detectors (31), signal processors, electromagnetic lenses (32), and image interpretation [see (33), for a complete review of the development of the SEM]. These improvements made possible the production of the first commercial SEM, the Cambridge Scientific Instruments Mark I "Stereoscan" (34). Although there have been remarkable advancements in the SEM since 1965, the SEM of today is very similar to its earliest predecessor. The most notable improvements are, an all digital interface, resolution of ~0.5 nm, a wide selection of electron and X-ray detectors, operation in the absence of a vacuum, and operation in the presence of condensing water vapor.

Parallel with the development of the SEM was the electron probe microanalyzer (EPMA), or simply, the electron microprobe. The designer of the EPMA, R. Castaing, intended to create an instrument that could measure the elemental

composition at a single point on a sample (35). To perform this task, a light microscope was used to observe the sample and to locate the position of a stationary electron beam. As the electron beam impinged on the sample, characteristic X-rays were emitted and intercepted by a wavelength dispersive spectrometer (WDS). By measuring the intensity of the X-rays and comparing them to that in a standard, Castaing was able to measure the concentration of a particular element in a given micron-sized location. As the SEM was commercialized, it became common to equip the EPMA with a SEM, in addition to the light microscope. The addition of the SEM allowed simultaneous high resolution imaging and elemental analyses. An additional new capability of the EPMA was that elemental maps of the sample surface could be produced. This capability extended the EPMA from a single point spectroscopic technique to an X-ray imaging electron microscope.

Although WDS has very good energy resolution ($<$1 to $\sim$10 eV, depending on the crystal used) and provides quantitative and highly sensitive ($>$10 ppm detection limit) measurements of elemental concentrations, the detection of X-rays by a diffracting crystal spectrometer (ie, WDS) is inherently inefficient. This results in relatively long analysis times, on the order of $\sim$1 min for major elements (ie, $>$10%) and $>$10 min to hours for trace elements (ie, $<$0.1 %). This and other drawbacks of the WDS promoted the development and proliferation of the energy dispersive spectrometer (EDS). As implied, the EDS measures the energy of the X-rays, and it does so in a parallel fashion, so that an entire elemental analysis of the sample is rapidly obtained (eg, 30–120). Although the energy resolution and detection limit are considerably lower for a typical EDS (130 vs 5 eV for WDS, and 0.5 vs 0.01 wt% for WDS), these parameters are quite acceptable for routine analysis. Advancements in EDS are continuing at a rapid pace and an experimental microcalorimeter EDS that measures the heat dissipated by an X-ray now provides a resolution of between $\sim$3 and 10 eV (36). The best WDS and EDS spectrometers can detect all elements heavier than lithium and analyze volumes as small as 10^{-12} cm^3. When operated at high energy resolution ($<$10 eV) these techniques can provide information about the valence state and structural environment of an ion. Given the great advantage of being able to correlate images of microstructure and microchemistry, it is extremely common to find EDS and to much lesser extent WDS detectors, installed on SEMs.

3.2. Transmission Electron Microscope. When Ernst Ruska produced the first TEM in 1929, the use of uv light and high NA condensers was the state of the art in light microscopy. Although the resolution of the TEM is limited by diffraction effects, as is the light microscope, the much shorter wavelength of electrons compared to visible light results in a $>$1000$\times$ increase in resolution. This resolution is in spite of the TEMs low numerical aperture (37). Ernst Abbe (1873) is credited for demonstrating that fine detail is resolved by an objective that includes within its angular aperture a direct beam of light and at least one of the diffracted rays from that detail. Because electrons have the properties of waves, Abbe's equation (eq. 1) therefore holds and may be used to calculate the theoretical resolution of the TEM. An excellent historical account of the beginning of transmission electron microscopy by Doane and co-workers (38) is available.

Due to the short mean free path of an electron in a solid, samples intended for TEM analysis need to be extremely thin, usually <300 nm, or else the material will not transmit the electron beam. The absolute sample thickness depends on sample density and the electron accelerating voltage used. TEMs are typically capable of producing a beam between 100 and 300 kV, however, there are several instruments that produce 3000-kV beams. TEMs are most commonly used in the conventional or "parallel beam" operation mode in which a relatively defocused beam, measuring several microns in diameter, is used to illuminate the sample. More advanced TEMs may employ a scanned beam mode in which the beam is focused to a diameter of <10 nm and is scanned over the area of interest in much the same way as any other scanning microscope (see the section SEM). Due to the very small probe sizes obtainable in scanning TEM (STEM), they are better suited for microchemical analysis and crystallographic studies. Most TEMs are able to resolve details of <0.5 nm on almost any substance. With this resolution, lattice fringes and rows of atoms are visible. TEMs may also be equipped with a wide variety of supplementary techniques (39). The most common are EDS, selected area electron diffraction (SAED) and electron energy loss spectroscopy (EELS). The EDS provides elemental information from X-rays. EELS measures the loss in kinetic energy of an ejected sample electron and from this determines the elemental concentration and, in some cases the valance state of the parent atom. SAED provides crystallographic information from diffraction patterns. One of the most recent advancements in TEM is the development of energy filtered TEM (EFTEM). The EFTEM allows the microscopist to specify the energy range of the electrons that will be used to construct an image.

TEM is widely used by biologists as well as materials scientists, although the high cost of a TEM ($250,000 to > $2,000,000) and the expertise required to utilize one limits usage. The most significant drawback to TEM are the sample thickness requirement and the ultrahigh vacuum (UHV) environment. Special cutting devices called "ultramicrotomes" are commonly used to cut soft materials into <500-nm sections, but sample preparation can still be very time consuming and frustrating. With that said, the TEM is still one of the most generally useful microscopes. Many thousands of TEMS are in daily use throughout the world. TEMs are applicable to the study of ultrafine particles (eg, pigments, abrasives and carbon blacks) as well as microtomed thin sections of plant and animal tissue, paper, polymers, composites, foods, industrial materials, minerals, etc Even metals can be made thin enough for detailed examination.

3.3. Scanning Electron Microscope. As with the TEM, the SEM achieves subnanometer resolution in spite of diffraction effects and a very low NA. As a consequence of the low NA, SEM images possess a much greater depth of field than optical images at the same magnification. Figure 9 shows the typical appearance of a SEM. The SEM consists of a column which houses the filament (ie, electron source), electromagnetic lens, and the beam scanning coils. At the base of the column is the sample chamber that contains the stage and detectors. A detailed view of the SEM column and the electron beam ray path is given in Figure 10. Depending on the goal of a particular investigation, the SEM may be operated in a number of different modes. These include high depth of field; low voltage, surface sensitive; high beam current and high

resolution modes. Several images that demonstrate the results obtained from these SEM modes are given in Figure 11.

Like other scanning microscopes, the SEM acquires data from the sample one point at a time. At each location where the electron beam impacts the sample, a flux of secondary electrons, backscatter electrons, X-rays, and other signals are emitted from the sample (Fig. 12). A portion of each signal travels in a direction such that it enters a detector (Fig. 13). The detector measures the intensity of electrons emitted at each point on the sample and converts this intensity value into a corresponding 8 bit (ie, 2^8, or 256) grayscale value. This digitized value is then displayed on a monitor (Fig. 14). The relative position of the output pixel on the monitor is synchronized with the movement and position of the beam on the sample. That is to say, when the beam is located at the position, row 1, column 1 (see Fig. 13), the intensity measurement from that point will be displayed in row 1, column 1 of the monitor. This image formation process applies to all of the collected signals and allows an image of each signal to be collected simultaneously. Given this image formation process, it is not difficult to understand that if the size of the raster is decreased (as in position **B** Fig. 13) then the magnification of the image will increase proportionally. For a complete discussion of nearly all aspects of SEM see (40).

In a modern digital SEM, all of the controls (eg, filament current, accelerating voltage, focus, magnification, stage control, EDS) are operated with the mouse, keyboard and a joystick rather than the numerous knobs, switches, and dials that decorated older analogue SEMs. The computer has also replaced the Polaroid camera, which had been used for image recording, and high quality digital images are now collected in just a few seconds. Computer control also allows sample positions to be preset into memory so that imaging and EDS analyses can be performed automatically. Many SEMs (as well as other microscopes) can also be viewed or operated from remote locations (eg, home, office, classroom) via the internet. This remote-control feature is excellent for teaching, technical consulting, or conversing with clients about their samples. The highest resolution SEMs utilize a field emission electron gun (FESEM) instead of a traditional thermionic emission gun. The FE gun produces an electron beam $\sim$1000$\times$ brighter, thus providing a higher signal-to-noise ratio, more rapid image and EDS acquisition, and a greater ability to collimate the electron beam. Improvements have also been made to the high voltage generator so that the accelerating voltage can be varied from as little as a few hundred volts to $>$30 kV in just a few seconds. This ability to operate at low voltage allows insulating materials to be examined with minimal charging. Furthermore, since different types of electrons may originate from different depths within the sample (Fig. 12), a voltage dependent contrast mechanism may be visible. For example, at 30 kV, BSEs are derived from a depth of up to 1000 nm whereas, at 1 kV and using a specialized in-lens or "snorkel" detector the SE^I signal is derived from a depth of $<$10 nm [see Fig. 12**b** and (40) for a discussion of SE^I vs SE^{II} electrons]. This increased degree of surface sensitivity in the SE^I images may allow the surface scientist or forensic detective to identify and study extremely thin surface coatings or contaminants that might otherwise go unnoticed.

The SEM can also be used to collect electron backscatter diffraction (EBSD) patterns and maps of crystalline samples. The contrast in EBSD is the result of

electron diffraction and channeling, and can be used to determine the crystallographic orientation of crystals to an accuracy of $<1^{\circ}$. EBSD maps obtained on polished polycrystalline samples (eg, alloys, rocks, ceramics) can provide a great deal of information concerning strain, recrystallization, creep, and other microstructural assessments.

The conditions of the specimen chamber during analyses have also been made much less restrictive in recent years. Both SEM and EDS can now be performed at atmospheric pressure and even in the presence of condensing water vapor. SEMs with this capability are generally referred to as environmental or variable pressure SEMs (ESEM or VPSEM) and require special detectors and chamber gases that prevent undesirable sample charging problems. VPSEM has already greatly increased the number of areas of application for SEM. These areas include biology, forensic science, environmental science, and other areas in which insulating, wet, or vacuum sensitive materials are routinely examined.

The SEM is very useful in any laboratory, but perhaps especially in the crime lab where a wide variety of materials are routinely examined. The possibility of confirming the common origin of evidence taken from a crime scene and a suspect has been demonstrated on countless occasions using SEM/EDS. The minor and trace element chemistry is different for most substances of the same bulk composition (eg, human hair, lead white pigments, and asbestos minerals). Each has a number of trace elements detectable by EDS or WDS and this approach can help to indicate or deny the possibility of common origin.

3.4. Scanning Auger Microscope. The scanning auger microscope (SAM) functions in much the same way as the SEM except that the conditions are optimized for the detection of Auger electrons. The SAM is usually equipped with a supplementary SE or BSE detector because the Auger signal is usually too weak for coarse positioning of the sample. Auger electrons are given off as electrons in outer shells cascade down to fill vacancies in the lower energy shells (41). Auger electrons retain their characteristic energies only if they have traveled less than a few nanometers within their parent material. This quality of the Auger electron guarantees that if they are detected, then they must have originated from no deeper than several nanometers within the material. For this reason, the images obtained from SAM and the chemical information obtained from Auger electron spectroscopy (AES) is of a highly surface sensitive nature. Auger electrons that travel greater than a few nanometers before exiting their material no longer have their characteristic energy. These electrons contribute to the rather large background (continuous radiation) signal.

A SAM can detect all elements except H and He and may have a spatial resolution equivalent to the FESEM ($\sim$0.5 nm), though most instruments do not have a resolution greater than $\sim$50 nm. Both SAM and AES are most commonly used in surface characterization and not for general microscopic imaging. Applications for SAM are mostly related to surface contamination and corrosion of metals and semiconductors. The high degree of chemical and structural specificity of an Auger electron allows the differentiation of elements in different bonding environments. For example, silicon as Si, SiO_2, SiO, or Si_3N_4 may be identified. Several of the disadvantages of SAM are charging by nonconducting

samples, localized destruction during depth profiling, complicated spectral interpretations, and the need for an UHV environment.

4. Scanning Probe Microscopy

4.1. History. The history of the SPMs is rather brief since the first STM was invented in 1981 (42). In 1986 two of the inventors of the STM, G. Binnig and H. Rohrer, were awarded one-half of the Noble Prize in Physics. The other one-half was given to E. Ruska, the late inventor of the first electron microscope. The STM is an extremely high resolution, and surface sensitive microscope capable of resolving single atoms. In addition to imaging surface microtopography, the STM may also image the current density at the surface or it may be used as a single-atom spectroscopic technique (ie, scanning tunneling spectroscopy, STS) to probe the density of states within the conduction and valence bands. While these abilities are unparalleled by any other microscope, the STM has one great disadvantage. It can only be used to image materials that conduct electricity. This disadvantage led to the rapid development of the second type of SPM, the AFM, which is able to image insulators as well as conductors (43). In the first 20 years of SPM there have been major advancements in image quality, image interpretation, and in the types of signals that may be imaged. Although the resolution of the STM is usually greater than the AFM, the ability of the AFM to measure a greater number of signals and collects image on nearly any material has led to its greater proliferation. Areas of application for SPM include semiconductor, metal and polymer processing and quality control, biological imaging, measurement of bonding or adhesive forces, magnetic imaging, nanolithiography, crystal growth and dissolution studies, and the identification of surface contamination and defects (44). Since the STM and AFM were developed in parallel they have very similar hardware and operating principles (Figs. 15 and 16).

4.2. Scanning Tunneling Microscopy. In STM, an extremely sharp metallic tip (typically composed of W or Pt–Ir) is extended toward a conductive surface until the distance separating them ($\leq$1 nm) is small enough to allow electrons to tunnel between the tip and sample (Fig. 17). The magnitude of the tunneling current is exponentially related to the tip-sample separation distance and is directly related to the bias voltage placed between the tip and sample. The exponential relationship allows for very precise measurement ($<$0.01 nm) and positioning of the tip in the Z direction (ie, the direction perpendicular to the sample surface). After a tunneling current has been established, the tip is rastered above the sample surface in an XY plane of known dimensions. As the tip is scanned it interacts with the electronic states (eg, electron orbitals) extending away from the surface atoms and may be driven toward or away from each atom by a piezoelectric scanner so that a constant height (ie, tip-sample separation) or constant current is maintained. Communication between the piezoelectric scanner and the current meter is by way of a feedback loop. This ensures that the tip does not crash into, or retract too far away from the sample. The resulting data of "tunneling current" or "height" as a function of the tip's XY position is plotted as a grayscale to achieve a microscopic image of the sample. SPM images typically show topographically high features as bright and low features are dark,

to resemble natural lighting. An atomic resolution topographic image of a FeS_2 surface is shown in Figure 17. The STM has been instrumental in the solution of questions concerning surface defects and atomic structure, eg, the 7×7 reconstruction of Si(111). Other applications include, surface diffusion and the observation of phase changes, and surface reconstructions at variable temperature and pressure.

4.3. Atomic Force Microscopy. AFM imaging is carried out in a manner related to STM. In AFM, the probe consists of a sharp tip (usually Si or Si_3N_4) grown on the underside of a flexible Si substrate called a cantilever. The cantilever has a reflective upper surface and may be in the shape of a triangle or narrow beam (often called a diving board) depending on the desired mechanical properties (Fig. 18). Before AFM scanning can be initiated, a beam of laser light is reflected off the end of the cantilever and aligned on the east–west line of a position sensitive photo–diode detector (Fig. 19). As the probe is scanned over the sample surface it will be deflected in the vertical or Z direction in response to the samples atomic forces. These atomic forces usually parallel the surface microtopography. The magnitude of the cantilever's Z deflection is measured by the change in the position of a laser beam on either side of the photodiode. This type of detection scheme is called an optical lever. The photodiode contains four quadrants, which may be paired to form north and south hemispheres or east and west hemispheres. In normal topographic imaging, the signal difference between the north and south hemisphere is used to measure the cantilever's deflection as described above. However, in lateral force mode (LFM, a.k.a. frictional force or chemical force) the signal difference between the east and west hemispheres is measured. This effectively measures the amount of torsion or twisting the cantilever experiences as it traverses a multicomponent or anisotropic sample. For example, consider a flat surface of rubber with intermixed chips of iron. As the tip crosses the interface between the rubber and iron the amount of cantilever twist or tip friction against the sample changes. Nanomechanical properties such as these cannot be measured by any other method. Another useful mode of AFM operation, called Lift Mode ™, involves the collection of twice as much data by recording measurements on the trace and retrace of each scan line. The trace or forward scan, usually records a topographic image. On the retrace or reverse scan, the probe is lifted off the surface by a user-defined amount and a far-field force such as a magnetic field is measured (Fig. 18d). This type of measurement requires that the tip be functionalized with a magnetic coating. Another common AFM mode is Tapping Mode™ (TMAFM). The TMAFM works in essentially the same way as described above, except that the probe is oscillated vertically ($\sim$20–100 nm) at its resonant frequency (8–500 MHz). Thus during a scan the tip actually lightly taps the surface. This mode of operation usually provides a topographic image except that the contact force is low enough so that delicate biological structures (eg, blood cells, DNA) can be imaged without tearing. A second type of TMAFM contrast is a phase image. In phase images, the contrast is a measure of the phase lag between the reference phase of the freely oscillating cantilever and the phase experienced as the tip taps a surface. The basic idea is that a soft or compliant material will cause a greater phase lag than a hard or stiffer material. Phase contrast can be extremely useful for identifying inhomogeneities in polymer films. A

final example of the SPMs versatility is its ability to be utilized under fluid. Figure 18c shows a flow through AFM fluid cell. This accessory allows one to observe crystal growth and dissolution, corrosion and hydration processes, often in real-time and at the atomic scale (Fig. 17b). New types of probe tips are constantly being developed to further expand the utility of SPM. Some of the most novel are a tip that emits a radio frequency so that micro nuclear magnetic resonance (nmr) imaging can be performed; a tip that contains a microscopic thermocouple provides spatially resolved thermal measurements as the sample is heated; and a tip fashioned from an optical fiber that makes possible near-field scanning optical microscopy (see section on NSOM).

Most SPMs utilize a low magnification ($<100\times$) light microscope to allow for precise alignment of the detection system and positioning of the SPM tip. Unfortunately, the light microscopes provided by the SPM manufacturers usually do not exploit the benefits of the many optical contrast-enhancing optical techniques discussed previously (eg, DIC, polarized light, fluorescence, etc). These techniques would allow more efficient SPM scanning and additional characterization data. To demonstrate this, a comparison is given of images obtained from the same location using AFM, SEM, and DIC (Fig. 20). It can be seen that the same nanometer sized steps visible in the AFM image are also resolved in the DIC image.

Despite the many capabilities of SPMs they have several weaknesses, including (*1*) low temporal resolution, eg, it may take anywhere from 5 seconds to 5 min to record a single image; (*2*) samples containing loosely bound particles, soft biologic material, moving subjects, sticky coatings, or treacherous microtopography may be difficult or impossible to accurately image; (*3*) image interpretation and troubleshooting can be difficult, especially for the inexperienced operator; (*4*) the maximum field of view is small, $\sim 100 \times 100$ μm and, (*5*) the morphology and sharpness of the probe may change during imaging, thus affecting the quality and resolution of the image. Furthermore, there can be uncertainty as to whether or not the SPM image obtained is a true representation of the sample.

4.4. Near-Field Scanning Optical Microscope. The NSOM is a combination of a light microscope and a SPM (45). However, unlike a conventional light microscope, the light being utilized is of fractional wavelength. By using a beam of visible light, the NSOM is the earliest of the probe scopes, at least in conception, and is another apparent exception to Abbe's diffraction-limited resolution rule. In NSOM, an aperture much smaller than the wavelength of light (and less than the diffraction limit) is used to illuminate an object. The resolution then is limited only by the size of that beam. To achieve this, light issuing from a very tiny aperture at the end of a glass capillary is scanned within a distance of $\sim\lambda/2$ from the surface. Resolution in the range of 10–20 nm has been achieved (46).

Although the idea on which NSOM is based goes back to 1928 (47), D. W. Pohl first believed it could be achieved with visible light and brought the concept to do it to fruition in 1984. There is considerable interest in NSOM and several commercial instruments are now available. A recent application involves using NSOM for localized absorption spectroscopy and fluorescence imaging of living cells (48).

4.5. Photon Scanning Tunneling Microscopy. PSTM is very similar to STM except that photons (ie, light) undergo tunneling rather than electrons. Although total reflection occurs when light strikes a higher index interface at greater than the critical angle, a short range electrical field extends a fraction of a wavelength through that interface, where it can interact with very near surfaces. Such electrical fields are termed evanescent waves. The photon intensity decreases exponentially away from the totally reflecting surface; hence, height variations in any surface within the evanescent wave range may be imaged (49). Commercially available PTMs have a lateral resolution of 160 nm and subnanometer vertical resolution. The nondestructive, instantaneous 3D viewing of a surface (no scanning) yields real-time imaging as one traverses a given sample. The sample must be a dielectric, but transparent polymer replicas of opaque samples can be studied.

5. Other Microscopes

5.1. Atom Probe Microscopy. Atom probe microscopy includes several related techniques that are based on the concept of field emission. Field emission (FE) is a phenomenon in which electrons may be pulled from a surface by a sufficiently high electrostatic field (50). To achieve a high enough field strength the sample (called an emitter) must be fashioned into a very sharp tip ($<$30 nm in diameter). This requirement severely restricts field emission techniques to metals. In a field emission microscope (FEM), as FE occurs the ejected electrons are propelled along the field lines into a fluorescent screen and produce a grayscale image representing the energy of the incident electrons. The origin of the contrast in the image is due to the materials work function anisotropy. The work function is the energy required to remove an electron from a material and into vacuum. Since the work function will vary depending on the crystallographic environment (ie, crystal plane) from which the electron originated, bright areas on the fluorescent screen will indicate a relatively low workfunction.

In the related technique of field ion microscopy (FIM), an ionizable imaging gas (eg, He, Ne, Ar) is exposed to the emitter. The gas and surface atoms are preferentially ionized at different surface sites depending on the localized field strength. Protruding atoms, adsorbed atom clusters, and ridges are commonly the sites of highest field strength. The resulting ions are accelerated toward a fluorescent screen and produce a direct image that is a representation of the atomic-scale distribution of the sites of ionization. The FIM, developed in 1955, was the first technique able to image single atoms (51). The FIM was later modified to allow chemical analysis of the emitted ions. This modification known as atomic probe FIM (APFIM), involves placing a mass spectrometer behind a hole in the fluorescent screen. This allowed the position and composition (ie, mass) of the emitted ions to be known (52). Most of the applications for FEM and FIM involve aspects of metallurgy (eg, grain boundary growth, diffusion, defects, identify single atom impurities) and theoretical studies of the electronic and atomic structure of surfaces.

5.2. X-Ray Microscopy. It has been recognized for nearly 100 years that the short wavelength of X-rays would provide an ideal light source for a

high resolution microscope. However, until recently the difficulties of focusing X-rays and the relative weakness of X-ray sources have frustrated efforts to reach this goal (50,53). The development of more intense sources (eg, plasma sources, soft X-ray lasers, rotating anodes, and synchrotron sources) has made possible highly effective instruments for both X-ray microscopy and X-ray diffraction on submicron samples. The major problem in focusing X-rays is that they do not posses a charge, and therefore cannot be deflected with electromagnetic fields. Focusing of X-rays may be accomplished using zone plates or by grazing incidence or multilayer reflectors.

There are three main X-ray imaging techniques: contact radiography, shadow projection X-ray microscopy, and scanning X-ray microscopy (SXM). Contact X-ray microradiography uses photographic film to map the presence of particular elements in a thin section of ceramics, rocks, etc. The method is still in use, but photoresist has replaced film as the detector. Two images are produced by X-rays from two different elemental targets, each having X-ray wavelengths on either side of a strong absorption edge of the element to be mapped. One of the two images shows particles or concentrated areas of the element; the other image shows no absorption of its characteristic X-rays and hence the same particles are barely, if at all, visible. Copper K α and cobalt K α X-rays differentiate concentrations of iron by differential absorption of the copper and cobalt X-rays as the imaging medium. It is most useful for detection of copper, nickel, cobalt, iron, manganese, chromium, and vanadium, although potassium, calcium, scandium, and titanium may also be detected. Submicrometer resolution is possible with high energy X-ray sources and poly(glycol methacrylate-ethyl acrylate) (PBS) resists.

Contact radiography has an interesting application. The sample, usually thin biological tissue, is placed on a clean PBS film and is exposed to soft X-rays for a brief amount of time. The X-rays cause the film to harden differentially, depending on the amount of absorption by the specimen. The resist is then "developed" using a solvent, usually 1:1 solution of methyl isobutyl ketone and 2-propanol, which leaves a surface relief image that can be examined by SEM, or TEM if thin enough. Although single atom imaging may never be possible with X-rays, the 10-nm region has already been resolved.

Shadow projection X-ray microscopy is a commercially established method used mostly by metallurgists to see partially through hot and molten metals up to $\sim$1 mm in thickness. In this technique, the material is heated to the point that a solid–liquid interface develops just a few microns under the surface. The X-ray beam is then focused at this interface and the portion of the beam that penetrates the sample is detected by a CCD camera. The X-ray opaque regions cause the appearance of a "shadow". This technique has a resolution of $\sim$1.0 μm.

The most advanced type of X-ray microscope is the scanning X-ray microscope (SXM). The SXMs utilize soft X-rays ($<$2 keV) with wavelengths of 1–10 nm usually generated from a synchrotron light source or rotating anode. The X-rays are passed through a monochromator and focused to a diameter of a few tens of nanometers using a zone plate. This parameter fixes and limits the resolution. In most instruments, the beam is stationary and the sample is rastered beneath it. A variety of detectors may be placed above and below the sample to image emitted signals such as, transmitted X-rays, visible fluorescence,

reflected X-rays, ejected photoelectrons, and Auger electrons. So far, it has been found that living material is only viable after short, low energy radiation doses. However, much information can be obtained from nonliving biological samples and inorganic materials. Aside from providing relatively high resolution, X-rays can be used with great sensitivity (up to 1000× more sensitive than electrons) to identify atomic concentrations and valence states.

A SXM that detects photoelectrons is called a microphotoelectron X-ray microscope (μXPS, a.k.a. microelectron spectroscopy for chemical analysis, μESCA). Commercial μXPS instruments utilize soft X-rays (typically, Al K α,1486 kev) while more expensive instruments utilize synchrotron radiation and are capable of operating down to X-ray wavelengths of <1 nm. μXPS is a highly surface sensitive technique, providing a depth resolution of just a few monolayers (2–10 nm). The surface sensitivity can be increased further by reducing the kinetic energy of the incident X-rays or by detecting the X-rays emitted from a grazing angle. Of course, there are tradeoffs, eg, a lower signal-to-noise ratio, longer analysis time, and fewer elements detectable. This degree of surface sensitivity is of great importance to understanding the properties of semiconductors and thin polymer films. Most of the SXM techniques are in a stage of rapid advancement. A detailed survey of most of these techniques is available (54).

5.3. Acoustic Microscope. In an acoustic microscope, a magnified image is formed using sound waves (50). The sound waves are typically generated using a piezoelectric (eg, ZnO) transducer that has been deposited as a film on the end of a cylinder of single-crystal sapphire. The other end of the sapphire cylinder (positioned directly above the sample) has had a spherical cavity removed from it so that when the acoustic pulse is propagated down the length of the cylinder it becomes focused by reflection, to a diffraction limited spot. To reduce the attenuation of the wave, the sapphire and sample are coupled by a fluid media, usually distilled water. A resolution of ∼1 μm is typically, however, a resolution of 15 nm has been achieved under cryogenic conditions. The greatest application for the acoustic microscope is in the nondestructive imaging of cracks, void, interfaces and defects within opaque objects such as metals, ceramics, polymers, etc. Other applications include the measurement of density, elasticity, and viscosity.

6. Acknowledgments

This article was adapted, with permission, from an earlier version by W.C. McCrone. His contribution to the article is gratefully acknowledged. The author would also like to thank G. Laughlin, G. Myer, and D. Stoney for their editorial suggestions.

7. Appendix I—Acronyms

AA angular aperture
AES auger electron spectroscopy

AFM	atomic force microscope
APFIM	atomic probe FIM
DIC	differential interference contrast
DOF	depth of field
EBSD	electron backscatter diffraction
EDS	energy dispersive spectroscopy
EELS	electron energy loss spectroscopy
EFTEM	energy filtered TEM
EPMA	electron probe microanalyzer
ESEM	environmental SEM
FE	field emission
FEM	field emission microscopy
FESEM	field emission scanning electron microscope
FIM	field ion microscopy
FTir	fourier transform infrared spectroscopy
HPSEM	high pressure SEM
ir	infrared
LFM	lateral force microscope
LSCM	laser scanning confocal microscope
MFM	magnetic force microscopy
MOLE	molecular orbital laser examiner
NA	numerical aperture
nmr	nuclear magnetic resonance
NSOM	nearfield scanning optical microscope
PBS	poly(glycol methacrylate-ethyl acrylate)
PLM	polarized light microscope
PPL	plane-polarized light
PSTM	photon scanning tunneling microscope
SAED	selected area electron diffraction
SAM	scanning auger microscope
SEM	scanning electron microscope
SERS	surface enhanced raman spectroscopy
SOM	scanning optical microscope
SPM	scanning probe microscope
STEM	scanning transmission electron microscope
STM	scanning tunneling microscope
STS	scanning tunneling spectroscopy
SXM	scanning X-ray microscopy
TEM	transmission electron microscope
TMAFM	tapping-mode atomic force microscopy
TSM	tandem scanning microscope
UHV	ultrahigh vacuum
uv	ultraviolet
VPSEM	Variable pressure SEM
WDS	wavelength dispersive spectroscopy
XPL	crossed-polarized light
μXPS	micro X-ray photoelectron microscope
μESCA	microelectron spectroscopy for chemical analysis

BIBLIOGRAPHY

"Microscopy" in *ECT* 4th ed., Vol. 16, pp. 651–672, by Walter C. McCrone, McCrone Research Institute; "Microscopy" in *ECT* (online), posting date: December 4, 2000, Walter C. McCrone, McCrone Research Institute.

CITED PUBLICATIONS

1. Selected microscopy journals: *Journal of Microscopy; Microscopy Today, Microscopy and Analysis; Scanning; The Microscope; Ultramicroscopy;* selected microscopy societies: Microscopical Society of America; Microbeam Society; The Royal Microscopical Society; State Microscopical Society of Illinois; State Microscopical Society of New York. Search online for additional microscopy resources, including listserves, courses, conferences, vendors, publications, techniques, etc.
2. P. M. Cooke, *Chem. Microscopy Rev., Anal. Chem.* **72**(12), 169 (2000).
3. C. W. Mason, *Handbook of Chemical Microscopy* 4th ed., John Wiley & Sons, Inc., New York, 1983.
4. S. H. Gage, *The Microscope*, Comstock, Ithaca, N.Y., (1908, 1917, 1920, 1925, 1932, 1936).
5. N. H. Hartshorne and A. Stuart, *Crystals and the Polarizing Microscope*, Edward Arnold, London, 1934.
6. R. M. Allen, *The Microscope*, Van Nostrand, New York, 1940.
7. E. Abbe, *J. R. Microscop. Soc.*, 790 (1883).
8. *Ibid.*, 20 (1887).
9. A. Köhler, *Z. Wiss. Mikr.*, 433 (1893); abstract, *J. R. Microscop. Soc.*, 261 (1894).
10. M. Pluta, *Advanced light microscopy*, Elsevier, Amsterdam, The Netherlands, PWN-Polish Scientific Publishers, 1988, Vol. **1,** *Principles and basic properties*, 1988; Vol. **2,** *Specialized methods*, 1989; Vol. **3,** *Measuring techniques*, 1993.
11. W. C. McCrone, L. B. McCrone, and J. G. Delly, *Polarized Light Microscopy*, McCrone Research Institute, Chicago, Ill., 1987.
12. C. C. Hoyt and R. Oldenbour, *Amer. Lab.* July, 34 (1999).
13. F. D. Bloss, *Optical Crystallography*, Mineralogical Society of America, Washington, DC, 1999, p. 239.
14. W. D. Nesse, *Introduction to Optical Mineralogy*, Oxford University Press, New York, p. 335, 1991.
15. Ref. 11, pp. 169–196.
16. G. H. Needham, *The Practical Use of The Microscope*, Charles C. Thomas, Springfield, Ill., 1958.
17. R. B. McLaughlin, *Special Methods in Light Microscopy*, McCrone Research Institute, Chicago, Ill., 1977.
18. Ref. 17, pp. 114–121.
19. J. S. Ploem, *Introduction to fluorescence microscopy*, Oxford University Press, Oxford : Royal Microscopical Society, 1987.
20. W. T. Mason, *Fluorescent and luminescent probes for biological activity : a practical guide to technology for quantitative real-time analysis*, Academic Press, London, 1993, p. 433.
21. C. J. R. Sheppard and D. M. Shotton, *Confocal Laser Scanning Microscopy*, Bios Scientific Publishers, Springer-Verlag, New York, 1997, p. 106.
22. V. I. Petrov, *Phys. Status Solidi A* **133**(2), 189 (1992).

23. D. J. Marshall, *Cathodoluminescence of Geological Materials*, Nuclide Corporation, Acton, 1988, p. 146.
24. W. C. McCrone, *The Particle Atlas*, Vol. V, (out-of-print); available on CD-ROM, McCrone Research Institute, Chicago, Ill. 1979, p. 1155
25. G. Turrell and J. Corset, *Raman Microscopy Developments and Applications*, Academic Press, London, 1996.
26. H. J. Humecki, *Practical guide to infrared microspectroscopy*, Practical spectroscopy series, V. 19, Marcel Dekker, Inc., New York, 1995, p. 472.
27. S. Inoué, *Video Microscopy*, Plenum Publishing Corp., New York, 1986.
28. S. Inoué, T. moue, and B. Gunning, *Amer. Lab.*, 52 (April, 1969).
29. M. von Ardenne, *Z. Tech. Phys.* **109**, 553 (1938).
30. V. K. Zworykin, J. Hiller, and R. L. Snyder, *ASTM Bull.* **117**, 15 (1942).
31. T. E. Everhart and R. F. M. Thornley, *J. Sci. Instr.* **37**, 246, (1960).
32. D.G. W. Smith, Ph. D. Dissertation, Cambridge University, 1956.
33. C. W. Oatley, *J.App. Phys.* **53**, R1 (1982).
34. R. F. W. Pease and W. C. Nikon, *J. Phys. E.* **42**, 281 (1965).
35. R. Castaing, Ph. D. Dissertation, University of Paris, 1951.
36. D. A. Wollman and co-workers, Superconducting transition-edge-microcalorimeter x-ray spectrometer with 2 eV energy resolution at 1.5 keV, http://www.boulder.nist.gov/div814/div814/pubs/downloads/microcal_papers/wollman99b.pdf, Contribution of the U.S. Government, not subject to copyright, 1999.
37. J. W. Stephenson, *Trans. R.M.S.*, 82 (1877).
38. F. W. Doane, G. T. Simon, and J. H. L. Watson, *Canadian Contributions to Microscopy*, Microscopy Society of Canada, 1993.
39. D. B. Williams, and C. B. Carter, *Transmission Electron Microscopy a Textbook for Materials Scientists*, Plenum Press, New York, 1996, p. 729.
40. J. I. Goldstein and co-workers, *Scanning electron microscopy and X-ray microanalysis: a text for biologists, materials scientists, and geologists*, Plenum Press, New York, 1992, p. 820.
41. D. Briggs, and M. P. Seah, *Practical Surface Analysis Volume 1, Auger and X-ray photoelectron spectroscopy*, John Wiley & Sons, New York, 1990.
42. G. Binnig, H. Rohrer, C. Gerber, and E. Weibel, *Phys. Rev. Lett.* **49**, 57 (1982).
43. G. Binnig, C. F. Quate, and Ch. Gerber, *Phys. Rev. Lett.* **56**(9), 930 (1986).
44. R. Weissendanger, *Scanning Probe Microscopy: Analytical methods*, Springer, New York, 1998.
45. P. Zhang and co-workers, *Crit. Rev. Solid State Mat. Sci.* **25**, 87 (2000).
46. E. Betzig and co-workers, *Science*, **251** 1468 (Mar. 22, 1991).
47. E. H. Synge, *Philos. Mag.* **6**, 356 (1928).
48. M. Hausmann and co-workers, *NSOM imaging of labelled mitotic and meiotic chromosomes, Microscopy and Microanalysis*, Vol. 48, 2001, pp. 9–11.
49. J. M. Guerra, *Appl. Opt.* **29**, 3741 (1993).
50. B. G. Yacobi, D. B. Holt, and L. L. Kazmerski, *Microanalysis of solids*, Plenum Press, New York, 1994, p. 460.
51. E. W. Miller, *J. Appl. Phys*, **27** 473 (1956); **28**, 1 (1957).
52. K. Hono, *Acta Mater.* **47**(11), 3127 (1999).
53. E. Burge, *Proc. R. Instr. C.B.* **64**, 137 (1992).
54. W. Meyer, T. Warick, and D. Attwood, *International conference on X-ray microscopy*, American Institute of Physics, Melville, 2000.

ROB WEAVER
McCrone Research Institute

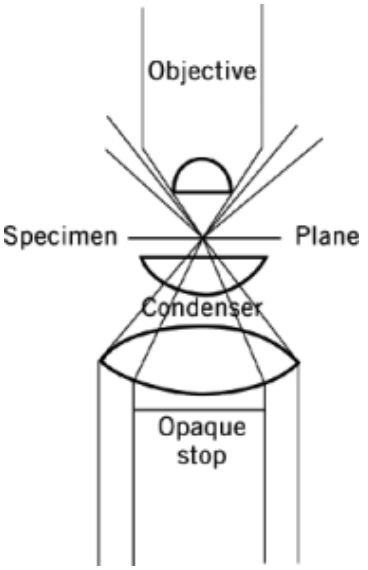

Fig. 1. Polarized light microscope with selected components labeled.

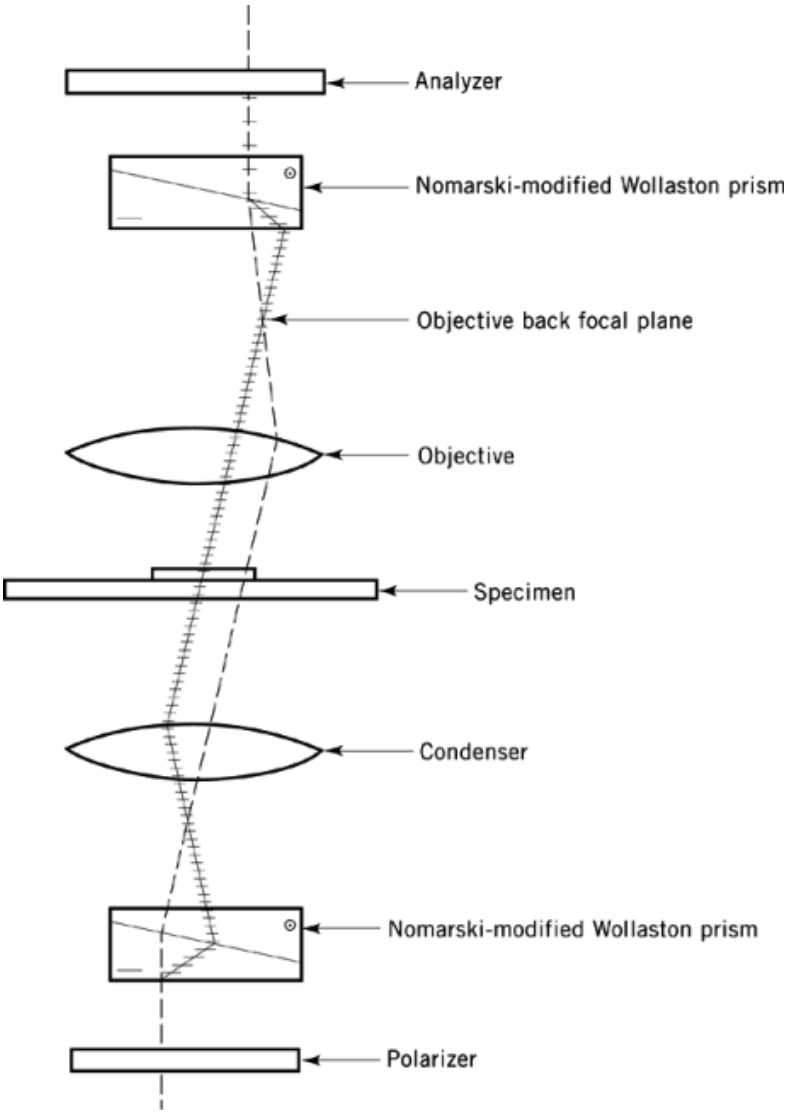

Fig. 2. Ray diagram and selected components of a reflected light confocal microscope. The lower portion of this figure also illustrate the inherent resolution and depth of field differences between a confocal (ie, point-source illumination) and a conventional (ie, full-field illumination) light microscope. In the case of a confocal microscope, only the in-focus rays (solid lines) are oriented to pass the confocal aperture and into the photomultiplier. These in-focus rays originate from a smaller thickness (and volume) within the sample (denoted as a black square) than do the out-of-focus rays (denoted by a light gray rectangle). As a result, the full-field microscope has a lower lateral resolution and greater depth of field, however, not all of the rays originating from this depth are in focus. Note that in a confocal microscope the beam is usually scanned across the sample. Three dimensional sample reconstructions are possible using a confocal microscope by combining images acquired at a different depths within the sample. Images taken at different levels within the sample are commonly referred to as “slices”.

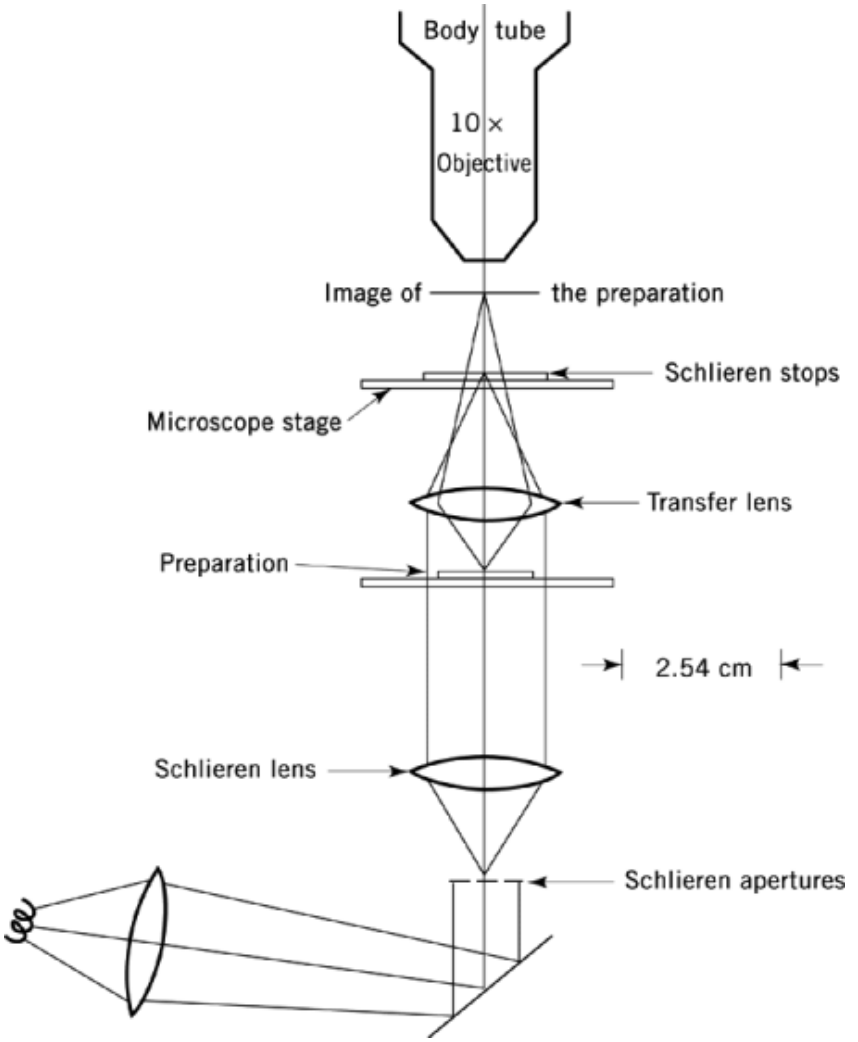

Fig. 3. The interaction of polarized light with an anisotropic crystal. Upon entering an anisotropic crystal a single ray of plane-polarized light is split into two polarized rays with their vibration direction perpendicular to each other. At position 1, where the ray enters the crystal, the two rays are initially in phase. However, since the rays travel at different velocities (oweing to birefringence, ie, the variation of refractive index with direction within the crystal), the faster ray (orange) will reach position 2 ahead of the slower ray (green). Thus, the rays develop a path difference or retardation as a result of traveling through the crystal. For simplicity, the incident light is shown as monochromatic and the fast and slow rays have been shown to be only two wavelengths long. The upper portion of the figure, above the break at position 2, shows the passage of the fast and slow rays through the analyzer. The analyzer is oriented so that only the component of the fast and slow rays with a north–south vibration direction may be transmitted. As these components pass through the analyzer they interfere to produce a range of intensities from maximum brightness (constructive interference) to black (complete destructive interference), depending on the orientation of the crystal. In the case of white light, interference of the fast and slow rays also produces interference colors which are used as a basis for identifying and characterizing materials.

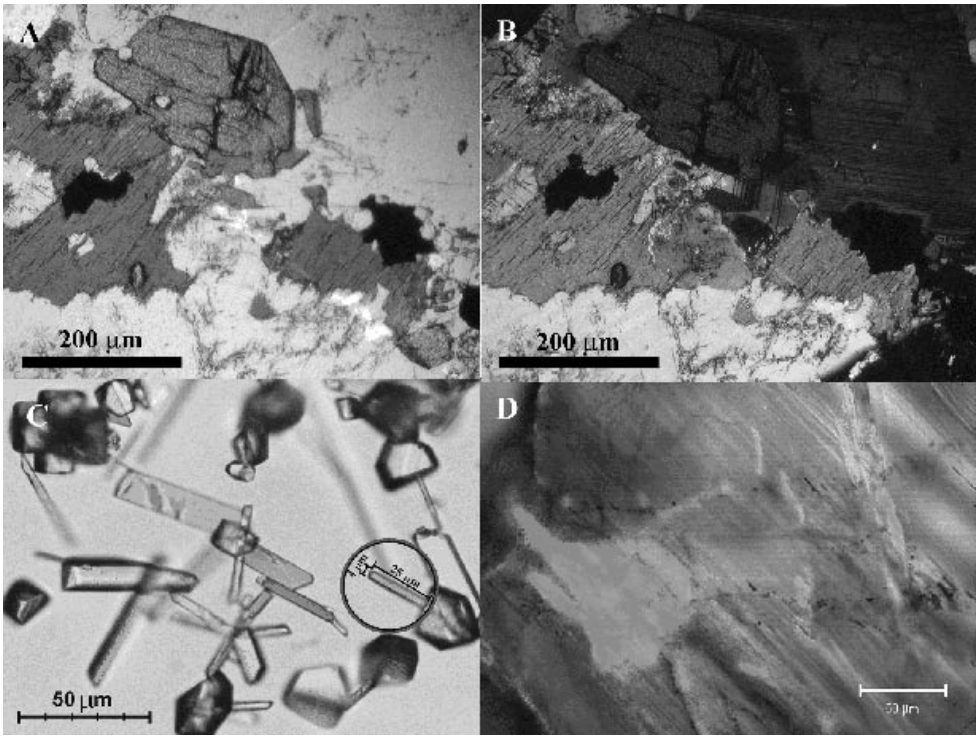

Fig. 4. (**a**, **b**) Transmitted light PPL and XPL images from the same area of a thin section of granitic rock. The color, opacity, microstructure, birefringence, and other optical properties can be used to identify these minerals and aspects of their geologic history. (**c**) Transmitted light PLM image of $Cd(NO_3)_2$ crystals. These crystals were formed as a result of a positive microchemical test for Cd. The crystal form, birefringence and other optical properties are diagnostic. The color is not the same for all of the crystals because they have different thicknesses and are in different orientations relative to the incident polarized light. A modest sense of the detection ability of PLM can be obtained by noting the size of the circled yellow crystal. The volume and mass are $\sim$400 μm^3 and $\sim$1.6 ng, respectively. (**d**) Reflected light LSCM image of diaspore (α-AlOOH) after exposure to siderophore (azotobactin) molecules. The siderophore is naturally fluorescent, having a peak absorption at 380 nm and a peak emission at 500 nm. The image was obtained in 0.5 s using a 364-nm uv laser as illumination and a 475-nm long pass filter. The false color blue shows the distribution of the fluorescent siderophore.

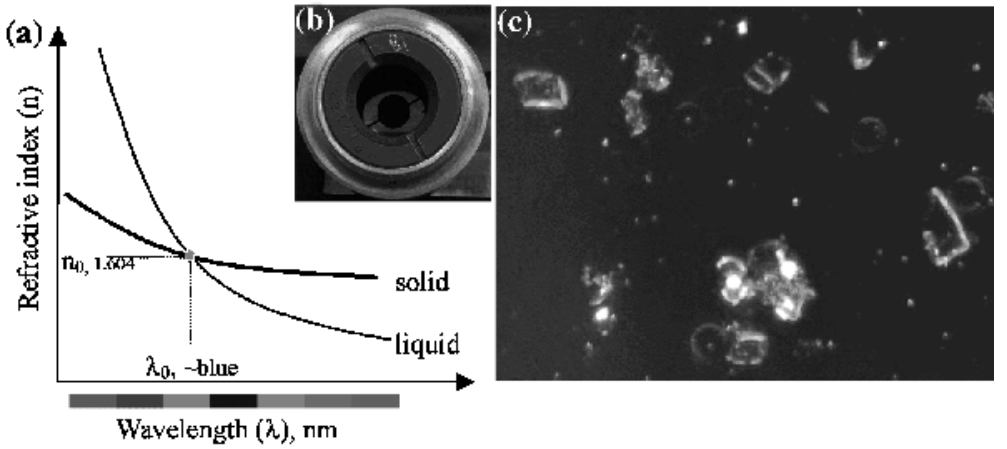

Fig. 5. The principles of dispersion staining. (**a**) Schematic dispersion curves for the liquid (Cargille, high dispersion liquid $n = 1.604$) and the solid (sodium bromate). The two curves cross at the wavelength (λ_o), in the blue part of the visible light spectrum. Since the index of refraction for blue light is the same for the solid and the liquid, the blue light will not undergo refraction at the solid–liquid interface and as a result it will travel straight up through the center of the objective and be absorbed by the central stop. (**b**) Photograph looking through a central stop dispersion staining objective. Note the circular opaque stop blocking the central part of the light path. (**c**) The resulting dispersion staining image. With the blue component removed from the white light the resulting image appears yellow, the compliment of blue, in locations throughout the sample where blue light was transmitted without undergoing refraction (i.e. mostly along the particle edges).

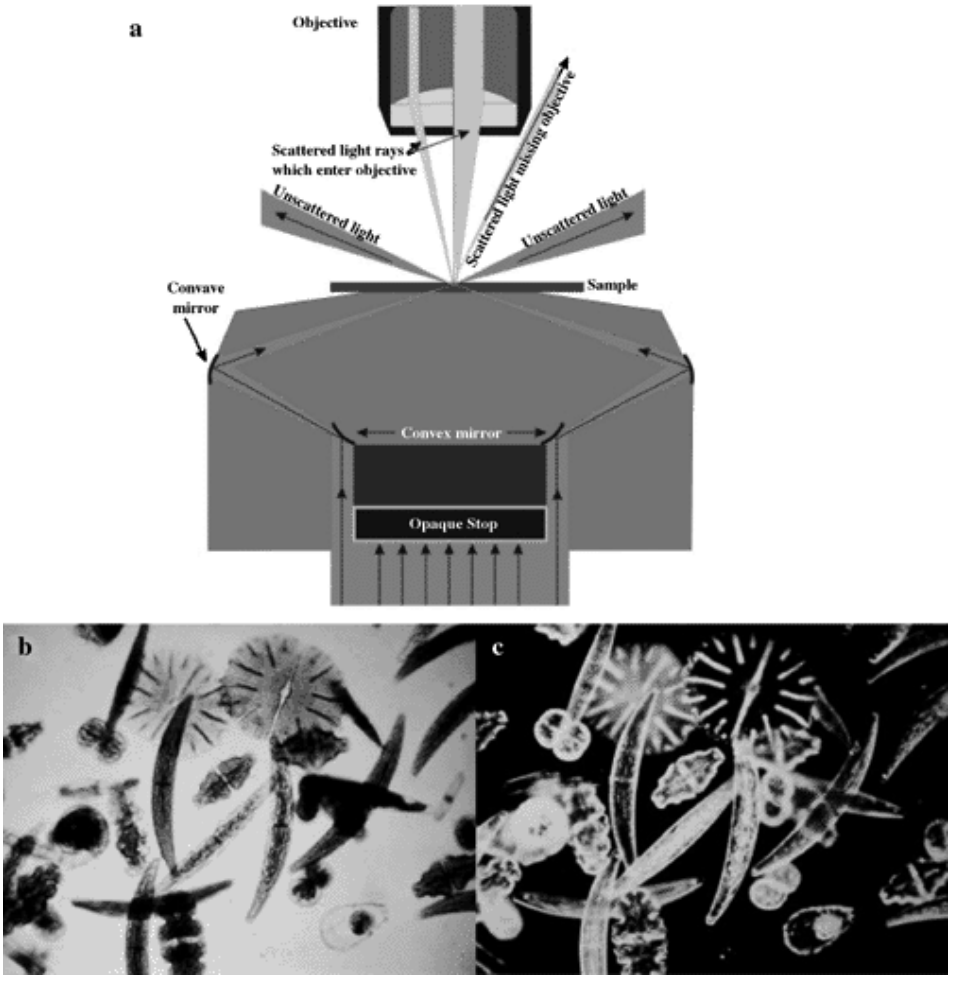

Fig. 6. (**a**) Cross-sectional view of a cardioid-type darkfield condenser and the associated ray paths. An opaque stop is used to produce a hollow cone of illuminating rays. Most of these rays that interact with the sample are not scattered upward into the objective. However, at some locations in a sample, usually at edges and interfaces, light may be scattered along a ray path that enters the objective and contributes to the image. (**b**, **c**) Brightfield and darkfield images from the same area of a desmids (freshwater algae) preparation. Note that the contrast in the darkfield image is primarily exhibited at interfaces and inhomogeneities.

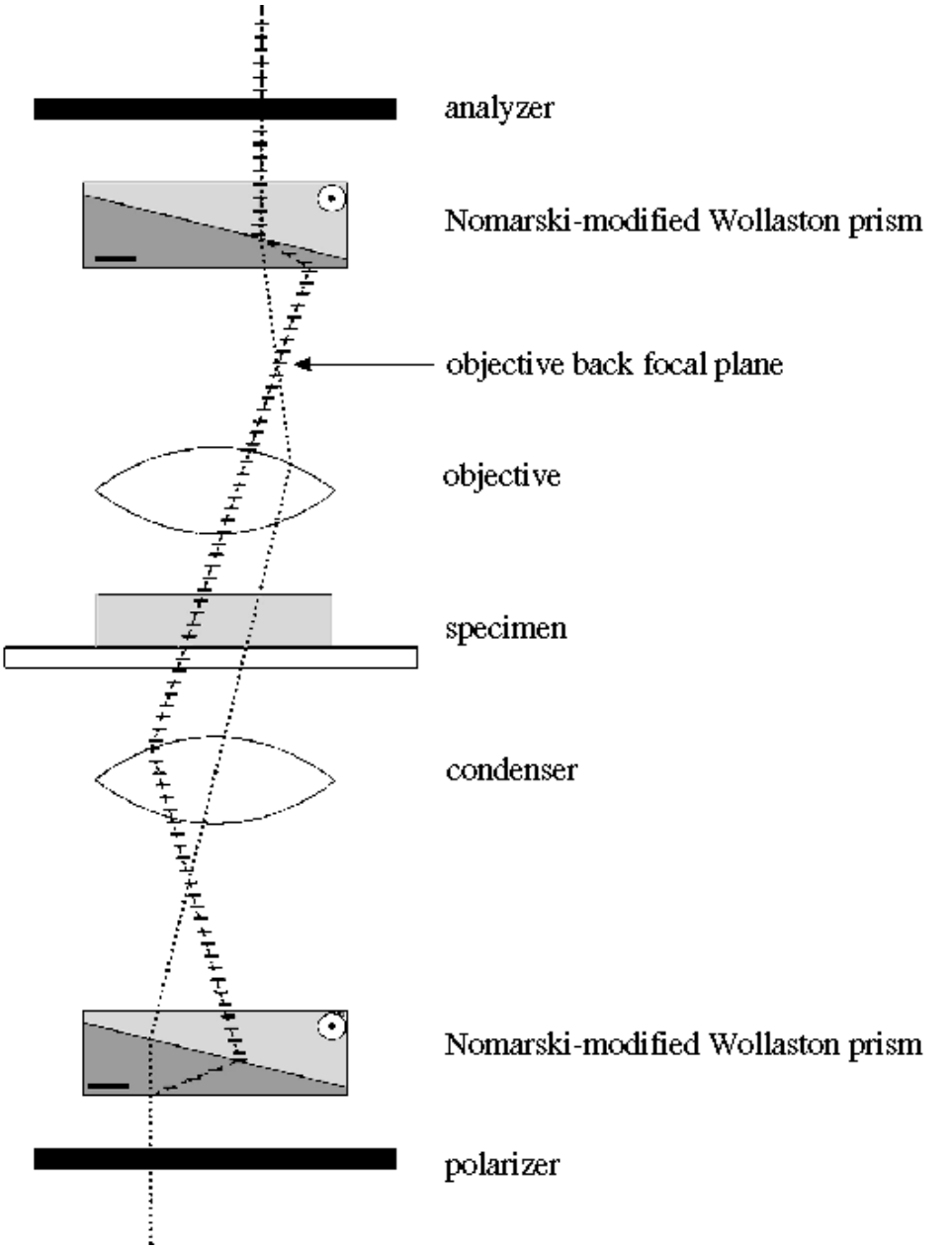

Fig. 7. Ray diagram for a Nomarski DIC microscope. The light paths shown are exaggerated. The Nomarski-modified Wollaston prism consists of two plates of calcite that have been cemented together with the fast and slow vibration directions oriented perpendicular to one another. The lower prism serves as a beam splitter while the upper prism recombines the beams after they have developed a path difference as a result of passing through the sample. In a reflected light, DIC system the upper prism serves as both the beam splitted and combiner.

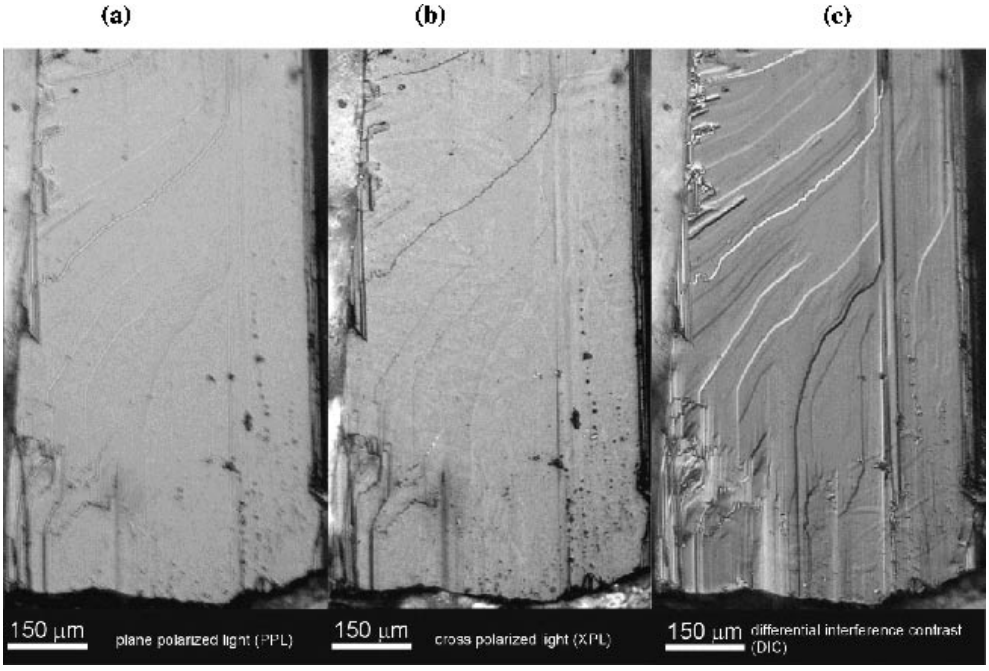

Fig. 8. Comparison of reflected light images of the (110) surface of manganite, γ-MnOOH as seen with, (**a**) PPL, (**b**) XPL and (**c**) DIC. In (**a**), the contrast and depth of field are quite low and the surface microtopgraphy is barely visible. In (**b**), it is apparent from the retardation colors that the surface contains two different crystallographic orientations. The blue domains are oriented 17° relative to the light gray domains. (**c**) DIC image showing the topographic offsets in high contrast and with a pseudo-3D shadow appearance. The smallest vertical offset resolved in this image is on the order of a few nanometers. This level of surface sensitivity is far superior to that seen in a SEM even when collected with an in-lens detector at 1 kV. Detection of topographic offsets using DIC even has advantages over SPM.

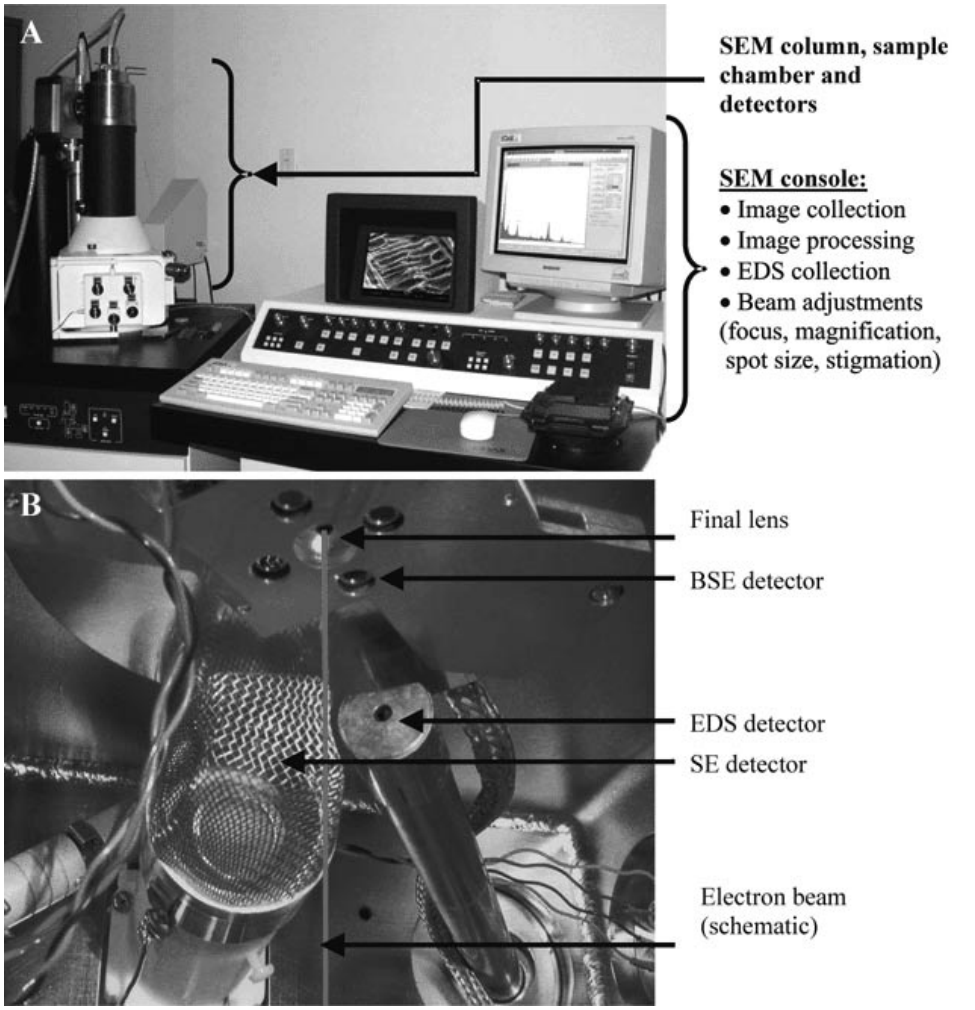

Fig. 9. (**a**) SEM column and console. A detailed schematic of the column is given in Figure 10. The monitors are used for displaying the specimen image and for collecting an EDS spectra. (**b**) A view of the inside of the SEM sample chamber showing the final lens aperture and the detectors. The sample is located just below this image.

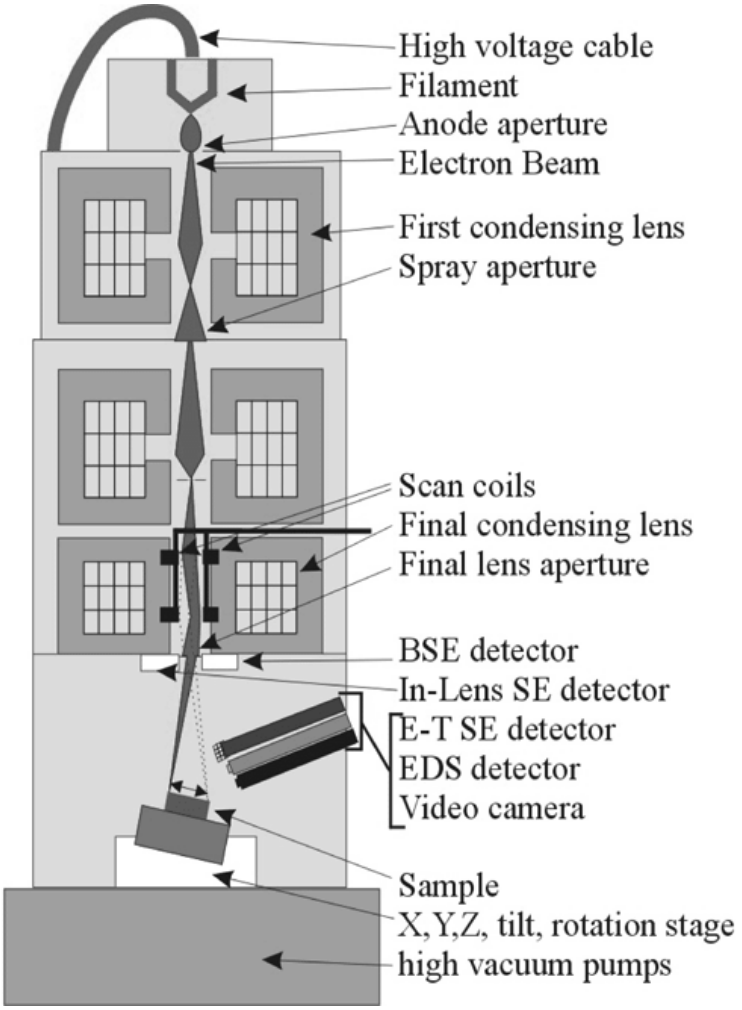

Fig. 10. Schematic illustration of selected components of a scanning electron microscope.

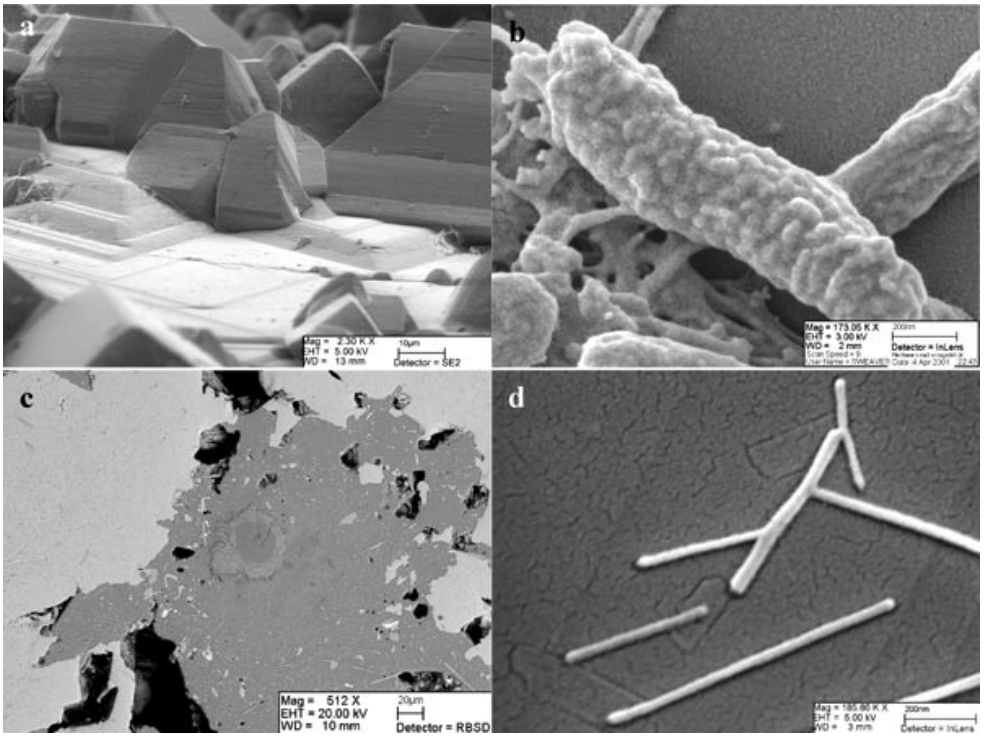

Fig. 11. SEM images illustrating the capabilities of the different imaging modes. (**a**) High depth of field mode showing the morphology of hematite (Fe_2O_3) crystals. (**b**) High resolution, low voltage, surface sensitive image of a bacteria and biofilm residing on a mineral surface. The lumpy surface texture of the bacteria is visible as are the nanometer sized droplets of the Au coating. (**c**) High beam current mode, backscatter electron image of the polished surface of a coin that has been corroded by exposure to seawater for over 100 years. The brighter areas are of higher average atomic number. (**d**) High resolution mode. Fibrous oxalate crystals precipitated on a Au film. Some of the crevices in the Au film are <2 nm wide.

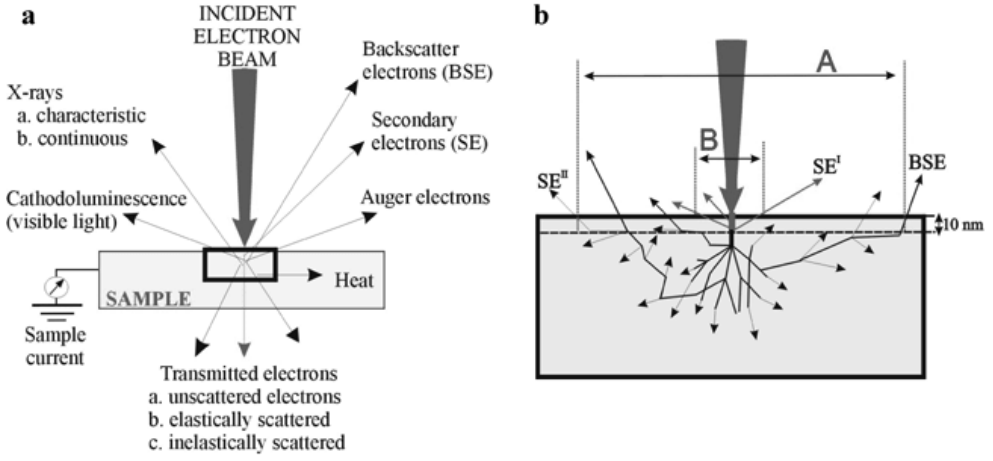

Fig. 12. (**a**) The various signals that may originate from a sample during exposure to an electron beam. In this illustration, the sample is shown as being sufficiently thin for the electron beam to be transmitted through it. This allows the figure to also illustrate the signals relevant to TEM. In general, a specialized detector is required to observe each signal. (**b**) Detailed view from (**a**) illustrating the production of two different types of secondary electrons, SE^{I} (red) and SE^{II} (thin black lines) and backscatter electrons, BSEs (thick black lines). SE^{I} type electrons are produced when primary beam electrons collide directly with sample atoms. Since primary beam electrons penetrate <10 nm into the surface, only a small portion of the total SE flux received by the detector is of the SE^{I} type. This relative portion can be increased to a significant level if the accelerating voltage of the primary beam is reduced to less than $\sim$3 kV. Above $\sim$3 kV SE^{II} and BSEs are the dominant imaging signals. The dashed line at a depth of 10 nm marks the maximum depth from which SE's may be created and still have enough energy to escape the solid and be detected. SE^{II} electrons are produced by collisions of backscatter electrons with sample atoms. Backscatter electrons are formed when primary beam electrons undergo elastic collisions with sample atoms that result in a $>90^{\circ}$ deflection from their original trajectory. Since BSEs possess relatively high energies they may originate from deep within the sample (up to $\sim$1 μm) depending on the density and composition. BSE's are usually a dominant component of any SEM image.

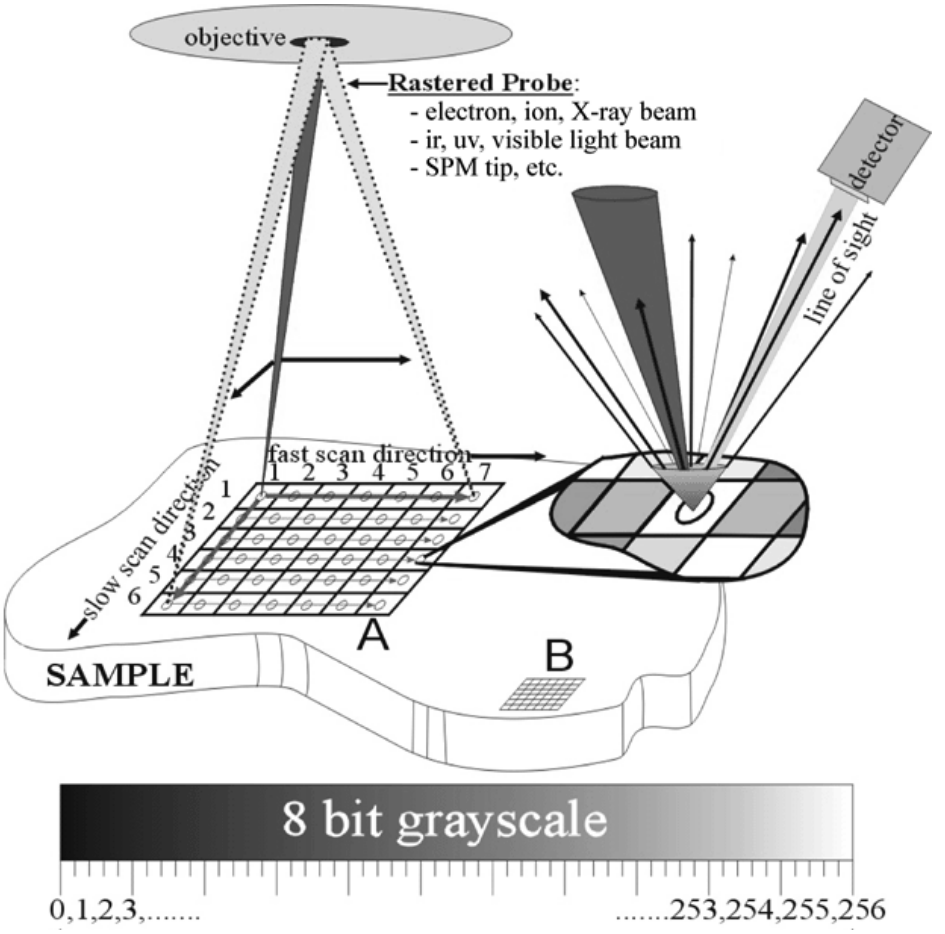

Fig. 13. Image collection process in a SEM. This general process of image formation is similar in other types of scanning microscopes (eg, LSCM, STEM, SPM). At each point in the XY scan the intensity of the emitted signal is measured, converted to an 8 bit (ie, 256 shade) grayscale value and displayed on the computer monitor. The successive measurement and subsequent display of adjacent data points (ie, pixels) creates the image. After a XY scan is complete the beam is deflected back to the position (1,1) and another scan is started. In order to increase the image magnification it is only necessary to decrease the area of the scan, as, eg, position B. To increase resolution however, the diameter of the probe must be reduced.

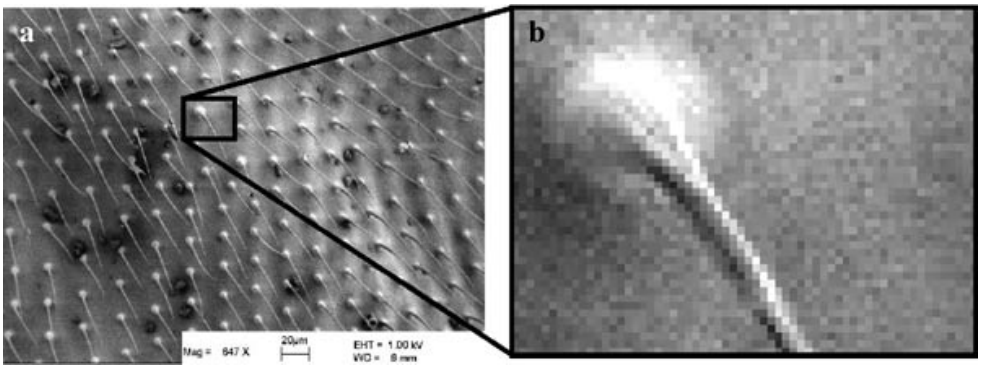

Fig. 14. (**a**) Low voltage FESEM image of the hairs on the wing of a housefly. The poorly conducting specimen is able to be imaged without charging due to the low accelerating potential of 1 kV. Although it is not apparent at this scale, image A is organized into 1024 rows and 768 columns of data points or pixels (ie, 786,432 pixels, or 0.78 megapixels). (**b**) Enlargement of the area outlined in (**a**) shows the individual pixels that comprise the image. The brightness of each pixel is proportional to the flux of the secondary electrons that originated from that point on the specimen. Perfect synchronization between the position of the electron beam on the sample and the output of that pixel value to the correct position on the computer monitor is required to produce an accurate image. Image (**a**) was collected in ~4 s. Thus, the SE detector collected data at a rate of 196,608 data points/s or, 0.25 frames/s). This rate is actually on the low end of a modern SEMs capability, but the image quality is still quite good.

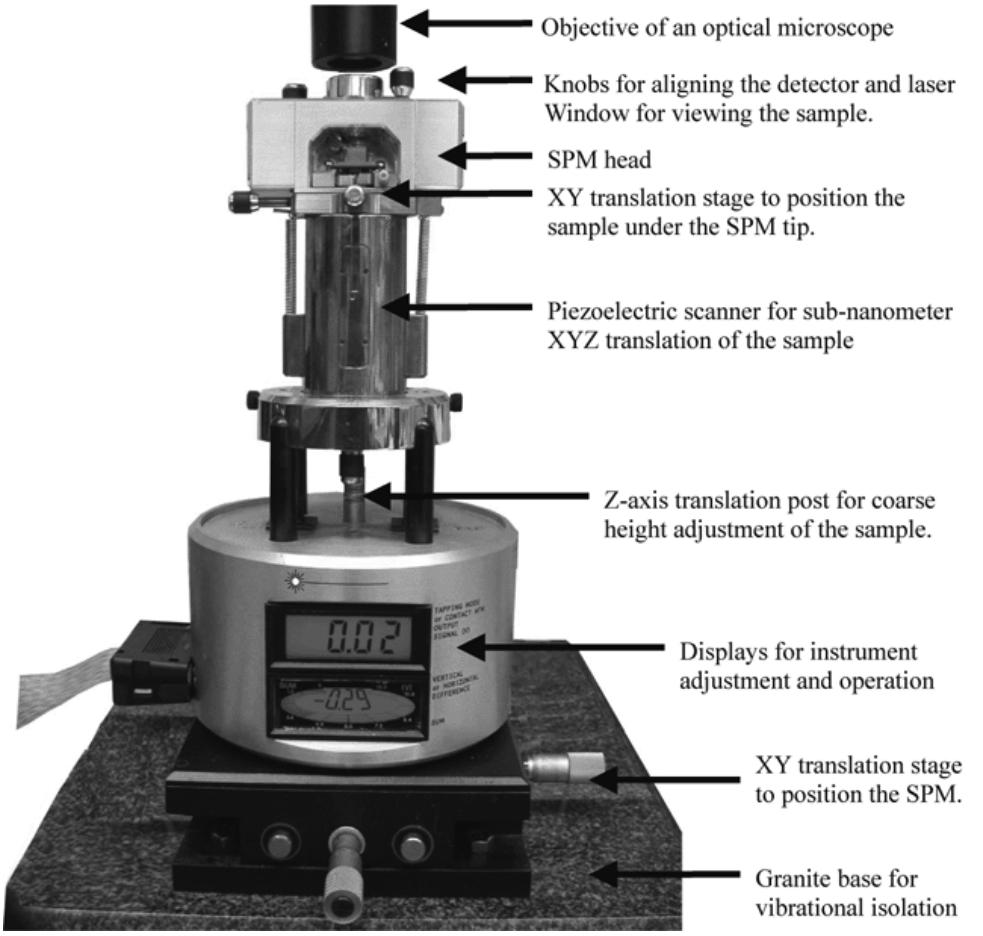

Fig. 15. A Digital Instruments Multimode SPM with selected components labeled. This instrument may perform all of the imaging modes of AFM and STM. The other two components of an SPM (not shown) are the electronics controller and the computer. The computer is used for digital signal processing, image processing and instrument control. See Figure 16 for a detailed view inside the SPM head.

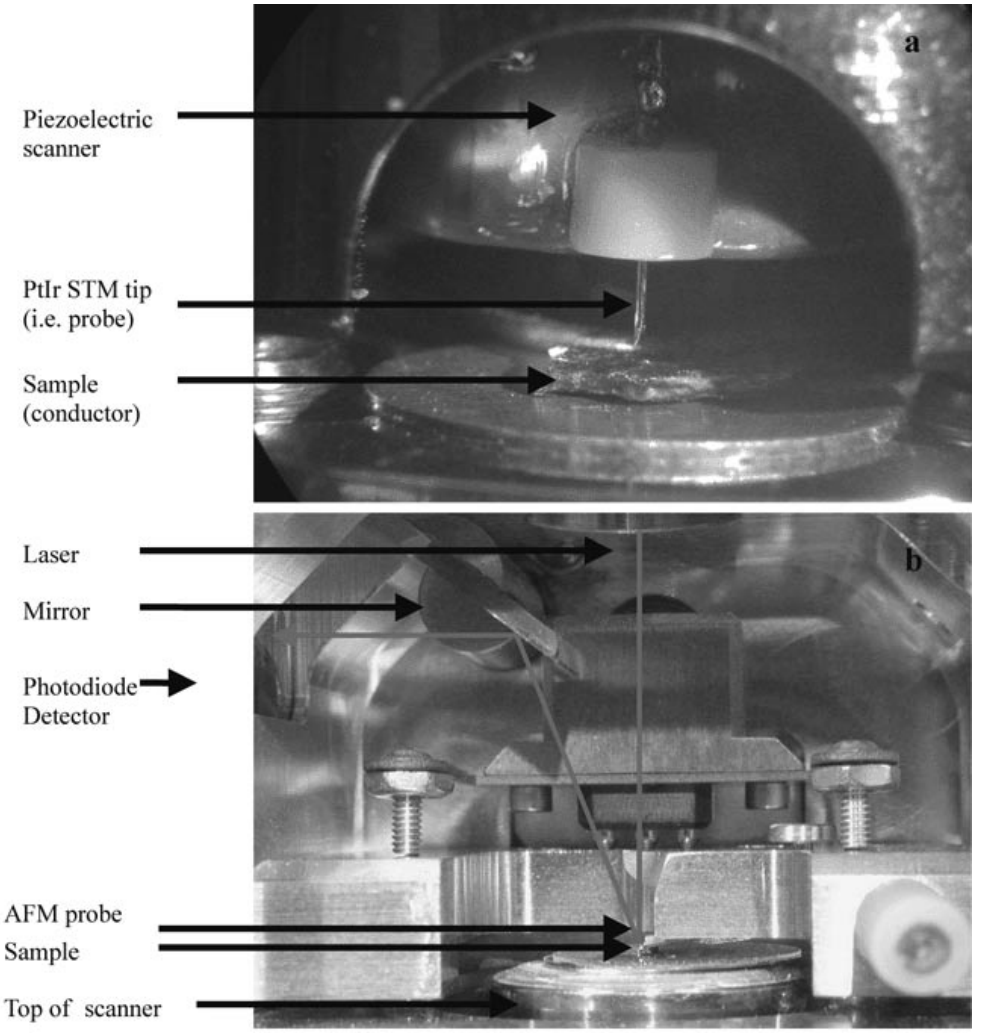

Fig. 16. Close-up views of the "heads" of a STM (**a**) and AFM (**b**). In both, STM and AFM a very sharp probe is positioned ~1 nm above a surface, and then scanned just above that surface. A feedback loop is used to provide communication between the tip and sample so that they do not touch. In AFM, the vertical motions of the cantilever are measured by an optical lever technique (see Fig. 17).

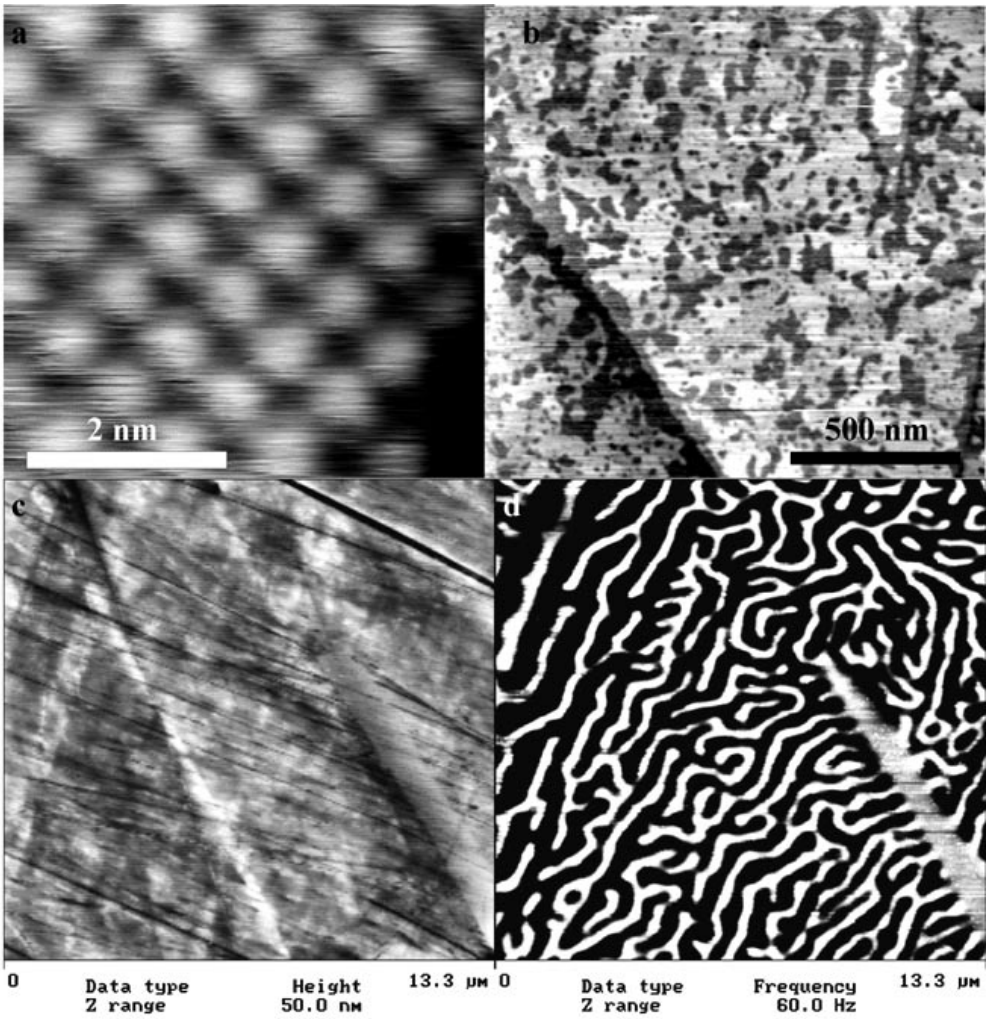

Fig. 17. (**a**) Atomic resolution STM image of FeS_2. Each bright spot represents an iron atom. The scale bar is two nanometers. (**b**) AFM image of γ-MnOOH collected during an in-situ dissolution experiment. Most of the etch pits (dark areas) are one monolayer in depth (~0.5 nm). (**c**, **d**) Topographic and magnetic force images of the same area on magnetite, Fe_3O_4, (111). The lineations on the surface in (**c**) are scratch marks produced during polishing. In **d** the alternating black and white pattern shows the distribution of the magnetic domains. The elongate white feature in the lower right is not magnetic and is visible in the topographic image(d).

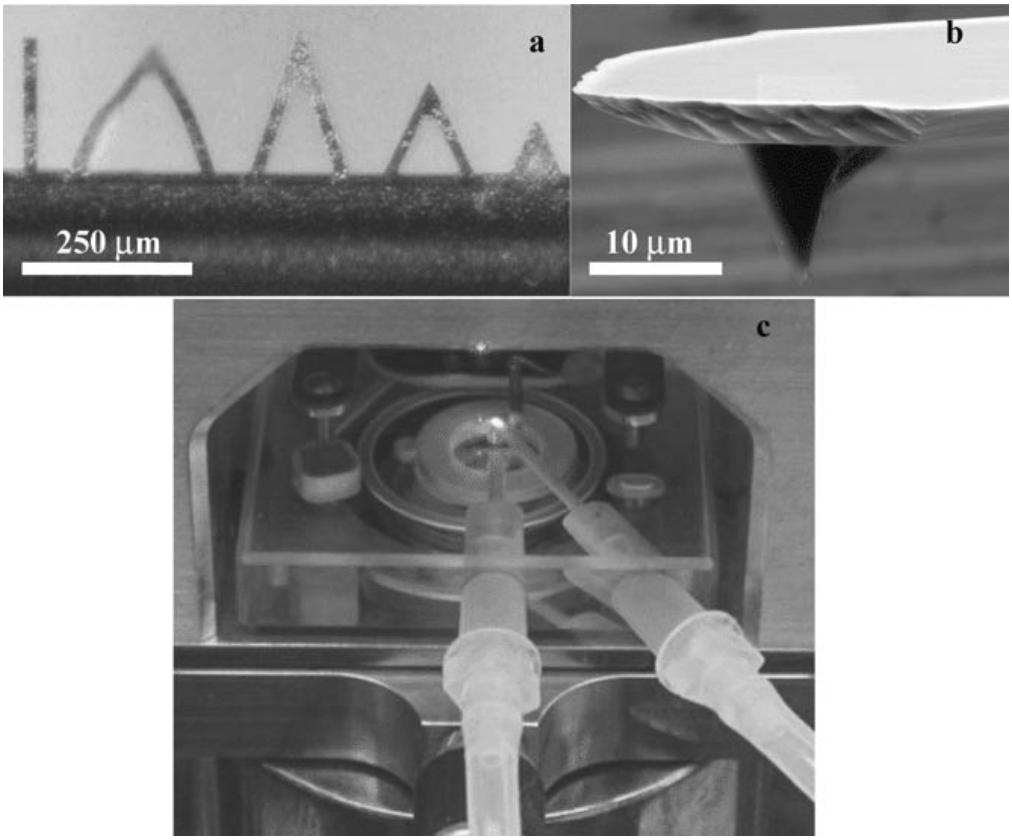

Fig. 18. Selected AFM components. (**a**) Commercially available Au-substrate containing five SPM probes. Depending on the SPM operating mode (eg, contact, Tapping, lateral force, fluid cell) the "single beam" or "triangular" shaped cantilever may be more appropriate. Each type of cantilever possesses a different spring constant (ie, stiffness) and may have a specialized type of tip (eg, sharpened Si_3N_4, magnetically coated silicon, chemically functionalized). (**b**) SEM image showing a profile view of a SPM tip. Before use, the radius at the apex of the tip is usually ~10–20 nm. The tip shown here has been used and actually has some debris adhering to it. This debris effectively increases the tip radius and lowers the ultimate resolution. (**c**) AFM head fitted with a fluid cell. The sample and probe are held immersed in an aqueous solution by the circular O-ring seen in the central region of the cell. In the front are the fluid inlet and outlet ports.

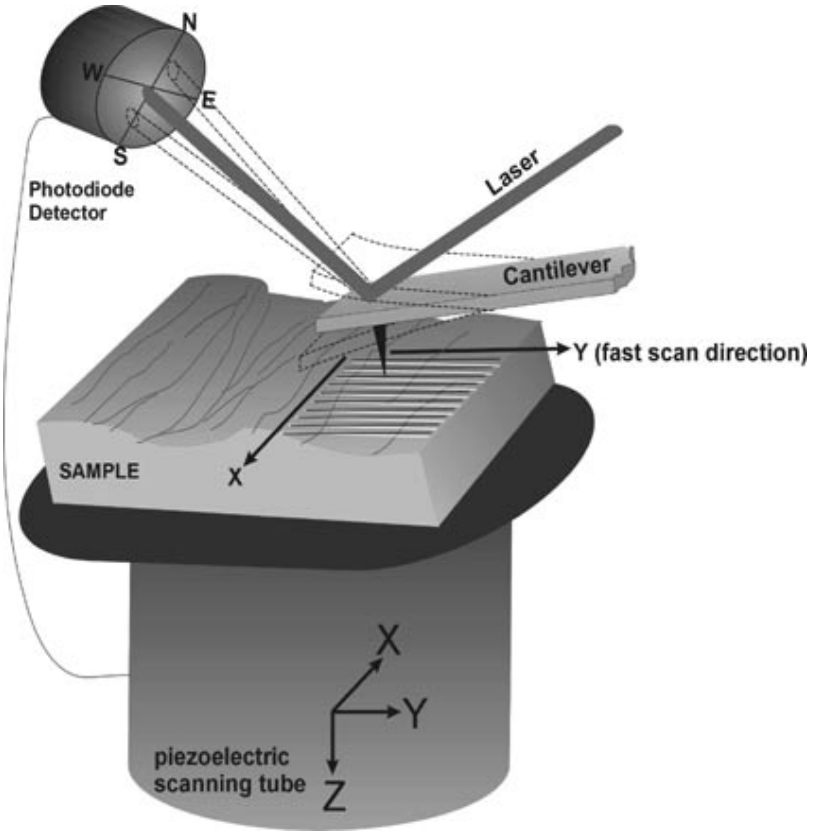

Fig. 19. Diagram depicting the optical lever detection and measurement scheme and the scanning process in a AFM. The dashed outline of the cantilever illustrates the extent of flexure it may undergo during an XY scan as it negotiates the sample's microtopography. As the cantilever is deflected up and down, so is the position of the laser light within the position-sensitive photodiode detector. By measuring the output signal across the north and south hemispheres of the detector, the relative position of the laser beam and thus the magnitude of the cantilever deflection can be measured. By plotting the Z (ie, vertical) deflection as a function of the tip's XY position, a 3 D topographic map of the sample surface may be generated. Three dimensional, subnanometer motion of the sample is provided by a piezoelectric scanner.

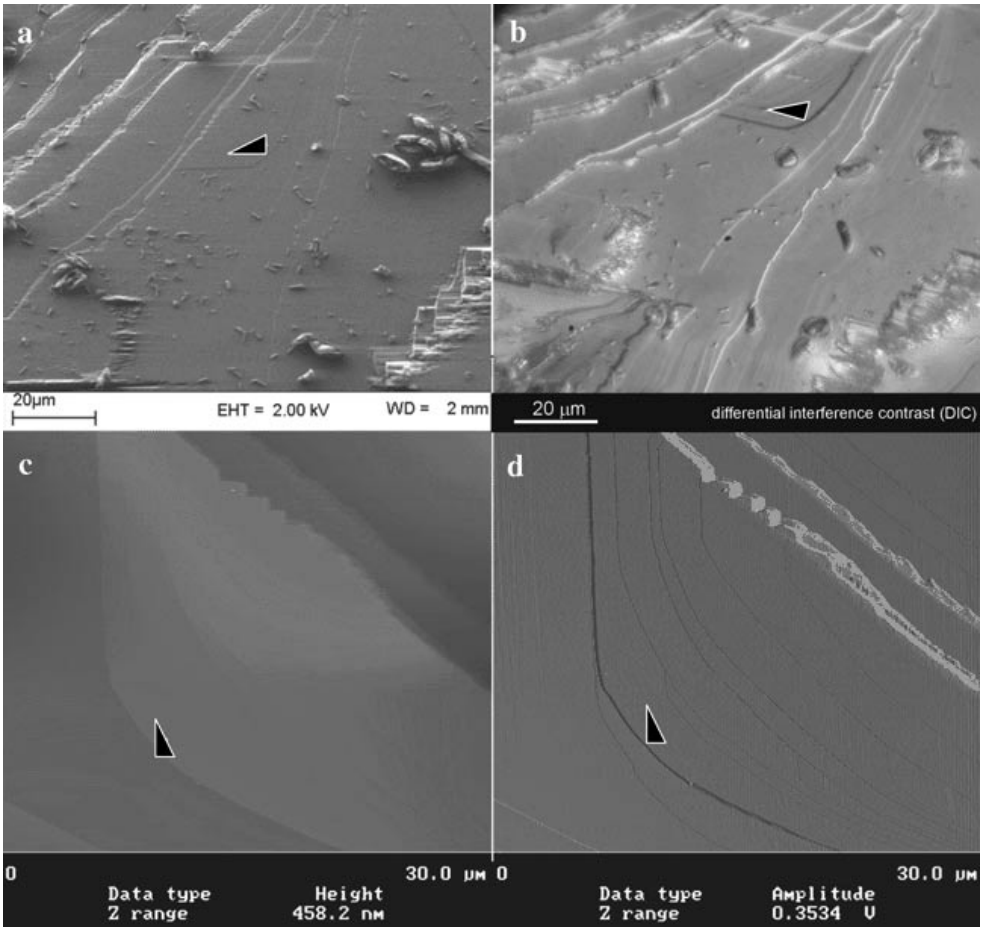

Fig. 20. A comparison of images obtained from approximately the same area using, (**a**) FESEM, (**b**) reflected DIC, and (**c**, **d**) AFM. The corresponding location and relative orientation of each image is marked with a triangle. Images (**a**) and (**b**) are approximately the same scale and orientation however, image (**b**) is rotated slightly clockwise of (**a**). Images (**c**) and (**d**) are at $\sim 4\times$ higher magnification and are rotated $\sim 90^{\circ}$ clockwise of (**a**). The contrast in (**d**) is the derivative of the topographic data in (**c**) and shows the step edges more clearly. The sample is a MnOOH crystal that has been exposed to microbes and algae. The subtle topographic steps located near the triangle are clearly resolved with DIC and AFM, but not SEM. The step heights are between 8 and 2 nm. Color is an obvious advantage to the optical image. The SEM image is entirely in focus whereas the optical image is slightly out of focus due to the lower depth of field.

Table 1. **A Comparison of the Three Most Common Types of Microscopes**

Microscopy type	Light	Electron	Scanning probe
basic pricinple	light is used to illuminate the sample, Glass lenses are used to focus and gather this light into a manified image. The image maybe directly observed through glass eyepieces (conventional) or the image may be presented on a point-by-point basis (scanning optical, SOM)	an electon beam is rastered across an area of the sample. At each sample position the beam resides, the flux of ejected secondary electrons is measured. The magnitude of this flux is instantly converted to a grayscale value and is displayed as a pixel on a monitor.	a sharp tip is scanned just above a sample surface. The electrical and atomic forces extending away from the surface are detected by a special probe. The detected signal is converted to a grayscale pixel value and plotted as a function of samples XY position.
lateral resolution	100–500 nm	0.1–3.0 nm	0.01–10 nm
vertical resolution	1 nm[a]–500 nm	5–20 nm	<0.1 nm
time resoltuion (ie, time required to collect a good image)	<1/1000 sec (conventional) <1 s to h (SOM), typically <30 s	<1 sec–4 min, typically <15 s	<1 sec–10 min, typically <2 s for atomic scale image, 2–4 min. for topograph mapping.
depth of field	good at low (<50×) magnification, poor at high manification (>200×)	usually excellent	excellent, provided all topographic positions are within the vertical travel range of the scanner (~10 μm)
characterization data	qualitative and quantitative metrology, optical properties, crystallographic data, noninvasive internal and external imaging	qualitative and quantitative metrology to the atomic scale, magnetic and crystallographic data, elemental mapping	quantitative metrology of surface phenomena related to chemical, magnetic, electronic, mechanical, etc, properties
advantages	usually provides enough data to unambiguously identify nearly any substance. May operate under almost any environment. Images are highly intuitive since they only require the sense of sight. Low cost.	excellent resolution and depth of field allows examination of nanometer-sized details. Elemental concentrations and crystallographic orientations may be quantitatively imaged.	provides 3D data at nanometer-scale resolution. Is surface sensitive to the upper monolayer. May operate under almost any environment.

Table 1. (*Continued*)

Microscopy type	Light	Electron	Scanning probe
disadvantages	resolution and depth of field are relatively low, analyses may be time consuming for the inexperienced operator.	not appropriate for examining living objects, on most systems it is difficult to image insulators	image acquisition may be quite slow, the image obtained may not accurately represent the sample, sample tilt and vibration will degrade quality
cost	$2–$60k (conventional) $50–250k (SOM)	$120–500k (SEM) $250–2000k (TEM)	$75–$250k

[a]A vertical resolution of 1 nm can be obtained using reflected light differential interference contrast (DIC). Lateral resolution is generally the same as the vertical resolution for non-opaque samples, unless special accessories (eg, DIC, confocal, etc) are used.

Table 2. **Ongoing Improvements Common to All Types of Microscopes**

1. Increase the spatial resolution (ie, lateral and vertical).
2. Reduce the amount of time required to collect an image. That is, increase the temporal resolution.
3. Lower the detection limit (ie, increased sensitivity).
4. Make the analytical environment less aggressive to the sample.
5. Develop new methods for sample characterization. That is, identify new imageable signals (ie, contrast mechanisms).
6. Reduce any undesirable interactions between the sample and probe (eg, local sample heating, desiccation, electrical charging, sample abrasion).
7. Design a more user friendly instrument with more capability for automation and less maintenance.
8. Reduce the amount of sample preparation.
9. Produce a more competitively priced microscope.

Table 3. **Resolution as a Function of NA and Wavelength (•)**

			Resolution, nm		
Objective	Mag.[a]	DOF[b]	NA	• = 550	• = 220
5×	50×	219.7	0.05	6700	2440
10×	100×	5.83	0.3	1100	410
20×	200×	1.90	0.5	670	245
40×	400×	1.00	0.65	515	190
40×[c]	400×	0.40	0.85	395	145
63×[d]	630×	0.12	0.95	355	130
100×[e] (water)	1000×	0.22	1.2	280	100
100×[e] (oil)	100×	0.15	1.4	240	90

[a]The magnification given is for a 10× eyepiece.

[b]The depth of field (DOF)= [•n $(n^2–NA^2)^{0.5}$]/NA^2; where, • = 550 nm (average wavelength for white light), n = the refractive index of the media between the objective and coverslip $n_{air} = 1.0$, $n_{water} = 1.33$, $n_{oil} = 1.5$)

[c]The standard 40× objective is the 0.65 NA (numerical aperture) version, rather than the higher resolution, but shorter working distance 0.85 NA objective.

[d]The highest obtainable numerical aperature for an objective used in air is 0.95.

[e]The NA of a water immersion objective is 1.2.